Macrophages utilize a bet-hedging strategy for antimicrobial activity in phagolysosomal acidification

Quigly Dragotakes[1], Kaitlin Stouffer[1], Man Shun Fu[1], Yehonatan Sella[3], Christine Youn[2], Insun Yoon[4], Carlos M. De Leon-Rodriguez[1], Joudeh B. Freij[1], Aviv Bergman[3,5,¥] and Arturo Casadevall[1,¥,*]

[1]Department of Molecular Microbiology and Immunology, Johns Hopkins School of Public Health, Baltimore, MD, [2]Department of Cellular and Molecular Medicine, Johns Hopkins School of Medicine, Baltimore, MD, [3]Department of Systems and Computational Biology, Albert Einstein College of Medicine, Bronx, NY, [4]Johns Hopkins University, and [5]Santa Fe Institute, Santa Fe, NM.

[¥]A.B. and A.C. share senior authorship

Running title: Chance contributes to host defense

Declaration of Interests

The authors declare no competing interests.

*Address correspondence:

Arturo Casadevall MD, PhD
Johns Hopkins School of Public Health
615 N. Wolfe Street
Room E5132
Baltimore, Maryland 21205

Abstract

Microbial ingestion by a macrophage results in the formation of an acidic phagolysosome but the host cell has no information on the pH susceptibility of the ingested organism. This poses a problem for the macrophage and raises the fundamental question of how the phagocytic cell optimizes the acidification process to prevail. We analyzed the dynamical distribution of phagolysosomal pH in murine and human macrophages that had ingested live or dead *Cryptococcus neoformans* cells, or inert beads. Phagolysosomal acidification produced a range of pH values that approximated normal distributions, but these differed from normality depending on ingested particle type. Analysis of the increments of pH reduction revealed no forbidden ordinal patterns, implying that phagosomal acidification process was a stochastic dynamical system. Using simulation modeling, we determined that by stochastically acidifying a phagolysosome to a pH within the observed distribution, macrophages sacrificed a small amount of overall fitness to gain the benefit of reduced variation in fitness. Hence, chance in the final phagosomal pH introduces unpredictability to the outcome of the macrophage-microbe, which implies a bet-hedging strategy that benefits the macrophage. While bet hedging is common in biological systems at the organism level, our results show its use at the organelle and cellular level.

Keywords (up to 10): Cryptococcus neoformans, Chaos, Bet-hedging, phagolysosome, trained immunity, chance, fungal, disease

Introduction

***Audaces fortuna iuvat* (Fortune favors the bold) - Virgil**

Phagocytosis is a fundamental cellular process used by unicellular organisms for nutrient acquisition as well as by host immune cells for microbial defense. The parallels between food acquisition and immunity have led to the suggestion that these two processes had a common evolutionary origin[1]. The process of phagocytosis results in the formation of a phagolysosome, a dynamic membrane bounded organelle, which represents a critical location in the struggle between the host and ingested microbial cells[2]. Microbial ingestion into phagosomes results in exposure to host cell microbicidal mechanisms, which leads to death for some microbes while others survive by subverting critical aspects of phagosome maturation and by damaging phagolysosome structural integrity.

The process of phagosomal maturation, encompassed by the fusion of the phagosome with lysosomes and lumen acidification, is a complex choreography that includes the recruitment of V-ATPase from lysosomes to the phagolysosome[2,3] and many other protein components[4]. Proton pumping into phagolysosomal lumen results in acidification that inhibits microbes and activates antimicrobial processes that are microbicidal. Consequently, some types of microbes, such as *Mycobacterium tuberculosis* and *Histoplasma capsulatum*, interfere with phagosomal maturation and acidification to promote their intracellular survival. The extent of phagosomal acidification is determined by numerous mechanisms that include proton flux through the pump, proton consumption in the phagosomal lumen, and backflow into the cytoplasm[5]. Phagosome acidification in macrophages is rapid with a pH of 6 being reached within 10 min after ingestion[6] and 5.4 by 15-20 min[7].

Cryptococcus neoformans is a facultative intracellular pathogen[8]. Upon ingestion by macrophages, *C. neoformans* resides in a mature acidic phagolysosome[9]. The outcome of macrophage-*C. neoformans* interaction is highly variable depending on whether the fungal cell is killed, inhibited, or unaltered. If not killed, *C. neoformans* can replicate intracellularly, resulting in variable outcomes which include death and lysis of the host cell, non-lytic exocytosis[10,11], transfer to another macrophage[12,13], or phagosomal persistence. A critical variable in determining the outcome of the *C. neoformans*-macrophage interaction is phagosomal membrane integrity, with maintenance of this barrier conducive to control of intracellular infection while loss of integrity leads to host cell death[14].

Prior studies of *C. neoformans* phagosomal acidification measured great variation in the pH of individual phagolysosomes[14–16]. The pH of cryptococcal phagolysosomes is affected by several microbial variables that include urease expression[15], phagosomal membrane integrity[14], and the presence of the cryptococcal capsule with glucuronic acid residues that can influence the final pH via acid base properties[17]. In addition, the capsule of *C. neoformans* increases in diameter as part of a stress response which can potentially

78 affect the phagolysosomal pH through increasing the phagolysosome volume, thus diluting its contents
79 and promoting membrane damage through physical stress[14].

80

81 In this study, we analyzed the time dependence of the phagolysosomal pH distribution in murine and
82 human macrophages and conclude that acidification is a stochastic process in which macrophages default
83 to a range of pHs with random variation. We demonstrate that, in doing so, macrophages employ a *bet-*
84 *hedging* strategy by sacrificing a small amount of overall fitness to ensure broad survivability. Thus, we
85 suggest that chance, in the form of stochastic dynamics, could be an important strategy in phagosomal
86 acidification, which benefits the macrophage by bet hedging against a range of pathogens, and could echo
87 through the immune process to introduce a fundamental uncertainty in the outcome of microbe-
88 macrophage interactions.

89

90 **Results**

91 We previously reported a wide distribution of phagolysosomal pH after the ingestion of *C. neoformans* by
92 murine bone marrow derived macrophages (BMDMs)[14,15]. Given that the growth rate of *C. neoformans* is
93 highly affected by pH[15,18] and that the outcome of the *C. neoformans*-macrophage interaction is
94 determined in the phagolysosome[14,19,20], we decided to analyze the distribution of phagolysosomal pH
95 mathematically to gain insight into the dynamics of the acidification process. Understanding the
96 fundamental process of phagolysosomal acidification, and if there are overarching rules or determinism
97 involved, could provide key insights to disease pathology of any pathogen, which would interact with the
98 phagolysosome. A scheme of the method used to determine phagosomal acidification with representative
99 data from polystyrene bead phagocytosis experiments are shown in Figure 1. To determine the pH of a
100 phagolysosome, particles are opsonized with an Oregon Green conjugated Ab. Oregon Green is pH
101 insensitive at Ex440/Em520 and pH sensitive at Ex488/Em520, allowing pH to be measured by quantifying
102 the ratio of fluorescent intensity between each wavelength. We were able to establish robust standard
103 curves from known pH controls and calculate unknown phagolysosome measurements (Figure 1B).

104

105 <u>Murine macrophage phagolysosomes acidify stochastically</u>

106 To determine whether phagolysosomal acidification is a deterministic or stochastic dynamical process, we
107 employed a permutation spectrum test[21] in which the distribution of ordinal patterns occurring in subsets
108 of our full dataset was analyzed (Figure 1C). Ordinal patterns simply refer to the order of each
109 measurement in terms of value, in our case the phagolysosomal pH, within a scanning window, which
110 parses all measurements within each condition, exemplified in Figure 1[22–25]. Here we found a 4-unit
111 window size to be the most appropriate. We found no forbidden patterns at any time evaluated for any
112 of the pH distributions resulting from the synchronized ingestion of beads, alive *C. neoformans,* or heat-
113 killed *C. neoformans*, which implies that the acidification is a stochastic process (Figure 2). A forbidden
114 ordinal is an ordinal pattern that does not appear during the time frame of our experiment. Despite the

115 overall population of macrophages showing chaotic dynamics, we considered whether the Chaotic
116 signatures occurred at the individual cellular level. That is, whether slight differences at the initiation of
117 phagocytosis propagated through maturation and acidification resulting in two phagolysosomes within
118 the same cell with different acidifications. To determine if this was the case, we analyzed the phagosomal
119 pH in pairs of bead containing phagolysosomes for which each pair was within a single macrophage. We
120 chose macrophages in which the ingested beads were visibly separated. We found that the differences
121 between phagolysosomal pH measurements of this cohort of phagolysosomes yields a normal distribution
122 centered at 0 with non-zero values, suggesting each individual phagosome has an independent target
123 phagolysosomal pH (SFig 1). The ordinal pattern analysis was repeated on several other strains and
124 conditions throughout the project and at no point did we observe forbidden ordinal patterns (SFig 2A),
125 again suggesting the process exhibits no signature of deterministic chaos[22–25]. Given that beads are inert
126 and cannot modify pH, we reasoned that their corresponding phagolysosomes would be the closest
127 approximation of a default acidification state and would therefore represent a "baseline" to which we
128 could compare phagolysosome acidification dynamics in other conditions.

129

130 Bead ingested murine macrophage phagolysosomes stabilize to a normally distributed pH

131 To probe the dynamics of the phagolysosomal acidification system at this baseline, we analyzed several
132 hundred individual phagolysosomal pH measurements at various time intervals after BMDMs had
133 ingested inert beads (Figure 3A). To determine whether phagolysosome pH measurements followed a
134 normal distribution, the measured relative pH values were fit to a predicted normal distribution using the
135 "fitdistrplus" R statistical package then analyzed via Q-Q plots and the Shapiro-Wilk normality test. We
136 found that phagolysosome pH value distributions did not approximate normality at early times (15 and 30
137 min), but mostly did at intervals of and past 1 h post infection. We were able to reject the Shapiro-Wilk
138 null hypothesis only at 15 min, 30 min, and 3 h (Figure 3B). We hypothesized that not all phagolysosomes
139 were fully mature before 1 h and reasoned that the bimodal appearance of pH at early time intervals is
140 likely due to the population of phagosomes being at different stages of maturity. Interestingly, the pH
141 distribution for the phagolysosomes containing live or dead *C. neoformans* did not approximate normality
142 even at later times. We rejected Shapiro-Wilk normality for each of these samples except for dead *C.*
143 *neoformans* at 3 h. Q-Q plots supported the notion that each sample skews further from normality
144 compared to bead ingested macrophage phagolysosome pH distributions (SFig 3). Considering that
145 macrophages default to a random pH from a particular normal distribution and that *C. neoformans* invest
146 in disrupting this process, we hypothesized that this system must confer some host benefit. Thus, we
147 decided to compare the pH distribution of mature bead ingested phagolysosomes to a range of pHs
148 tolerated by relevant potential pathogens.

149

150 Acidification Dynamics are Closely Related to Maturation

151 To probe whether the observed normality and stochasticity is a result of dynamics in acidification or in
152 the maturation process, we analyzed the intensity of two phagolysosomal maturation markers, EEA1 and

153 V-ATPase, over the same time course. Using relative intensity of each immunofluorescent staining as a
154 surrogate measurement of maturation, we found that, again, no samples had forbidden ordinal patterns,
155 suggesting phagolysosomal maturation, when measured by the accumulation of these markers, is also
156 stochastic in nature (SFig 4). However, neither of the fluorescence intensity measurements from these
157 markers approximated normality at any time, with sufficient skewing to reject the Shapiro Wilk null
158 hypothesis (SFig 5). Skewing of these measurements away from normality could reflect cytoplasmic
159 speckling, limitations of fluorescent microscopy resolution, non-linearity of fluorescence signals and the
160 inherent complexity of such a system, such that we are not confident to reject the notion that these
161 processes indeed demonstrate a normal distribution. We hypothesized that macrophages may experience
162 limited resources in terms of the number of available V-ATPase pumps at any given time and that we
163 might see a correlation between intensity of VATP staining around individual phagosomes in cells that had
164 ingested one versus multiple beads. We found no evidence of a correlation between V-ATPase staining,
165 or EEA1 for that matter, and total number of ingested particles (SFig 6).

166

167 BMDM phagolysosomes acidify to a pH range suboptimal for growth of soil and pathogenic microbes

168 The pH of soils varies greatly from acidic to alkaline based on a variety of conditions that, in turn,
169 determine the associated microbiome[26]. Soils contain many pathogenic microbes including *C.*
170 *neoformans*. Since the phagolysosome is an acidic environment, we reasoned that microbes that thrive in
171 acidic soils could proxy for the types of microbes that hosts, and thus macrophages, could encounter, and
172 pose a threat to the cell/host due to their acidophilic nature (ex. *Cryptococcus neoformans*). Hence, we
173 compared[27,28] the distribution of pH values from mature phagolysosomes (HPI ≥ 1 h) which had ingested
174 latex beads, as a measure of the range of acidities generated in the absence of microbial modulation,
175 relative to published soil microbe growth data as a function of pH (Figure 4). The latex bead pH distribution
176 is narrow and centered at a pH of about 4.5, which corresponds to a pH that significantly reduces the
177 optimal growth even for microbes in acidic soils. To generate a more relevant comparison to human
178 disease models, we also searched out the pH tolerance of 27 significant human pathogens which
179 macrophages are likely to encounter during human infectious diseases (Supplemental Table I). We then
180 compared these distributions to the pH distribution in bead ingested macrophage phagolysosomes (Figure
181 4). The distribution of this default macrophage pH heavily overlaps with the more inhibitory pH regions
182 when compared to both soil and known pathogen pH tolerances. Taken together these data suggest that
183 the low phagosomal pH is itself a defense mechanism, with a distribution that manifests bet hedging by
184 defaulting to a range, rather than single value, inhibitory to most of the spectrum of pathogens the
185 macrophage is likely to encounter.

186

187 Simulations of macrophage populations show stochastic pH as a bet-hedging strategy

188 Bet hedging is generally understood as a strategy whereby an organism decreases variation in fitness at
189 the expense of a small decrease in mean fitness. To test whether variation in macrophage phagolysosome
190 pH constitutes a diversified bet-hedging strategy, we first modeled host survival rate as a function of final

phagolysosomal pH in the context of a pathogen randomly selected from Supplemental Table I. This analysis modeled phagolysosomal pH as a normal distribution with mean μ and standard deviation σ varied over a range of possible values in order to test how bet hedging depends on these parameters. To each phagolysosomal pH, we associated a fitness value which models survival likelihood against pathogens, using the list of pathogens (Table 1), with their viable pH ranges collected from the literature, and we computed the distribution of fitness (p) as phagolysosomal pH varies (Figure 5A,B). As expected in bet hedging, we observed decreases in standard deviation of fitness with increasing σ of phagolysosomal pH (Figure 5C). Mean fitness was mostly unchanged with changing standard deviation, such that even in the most extremes deviations in phagolysosomal pH there were only slight changes in fitness in either direction.

Another way to formalize the emergence of bet hedging as an evolutionary strategy is by considering the average long-term rate of growth. Thus, we considered a multiplicative model, in which the growth rate (r_T) over a span of time (T) is defined as the geometric mean of $\rho_1, \dots, \rho_T$, where for each t ranging from 1 to T, ρ_t is the fitness at time t. Taking logs, log(r_T) is the average of log(ρ_1),…,log(ρ_T). By the law of large numbers, if we assume each ρ_t is independent and identically distributed, this average will approach E(log(ρ)). Thus E(log(ρ)) is the operative quantity to be maximized, rather than E(ρ). Note that applying the log transformation has the effect of placing heavier penalties on fitness values that are close to 0, so that maximizing mean log fitness will tend to encourage lower standard deviation in fitness[29]. Thus, increased mean log fitness is another indication of bet-hedging which directly relates to long-term growth. We indeed observe increased mean log fitness with increasing σ of phagolysosomal pH (Figure 5D).

To probe whether our simulations would reflect biological responses, we analyzed macrophage phagolysosomal pH in which cells treated with Chloroquine, a weak base that localizes to the phagolysosome. According to our model the increased shift in mean pH from chloroquine would result in a lower overall mean log fitness as a result of shifting the mean pH closer to 6, a more tolerable region for most of the candidate pathogens. Thus, we compared previously reported data[9] of *C. neoformans* containing phagolysosomes treated with chloroquine to our data from the respective time interval and found that chloroquine treatment results in a drastically reduced overall mean log fitness (-5.323) compared to the mean log fitness of our non-chloroquine treated data of the respective condition (-2.486).

Time intervals from ingestion of *C. neoformans* to initial budding are stochastic

C. neoformans replication rate is highly dependent on pH[15]. Consequently, we hypothesized that if phagolysosomal acidification followed stochastic dynamics, this would be reflected on the time interval from ingestion to initial replication. Analysis of time intervals to initial fungal cell budding events revealed stochastic dynamics with no evidence of forbidden ordinal patterns (SFig 2B). Similar results were observed for initial budding of wild type and urease negative strains of *C. neoformans*, which reside in phagolysosomes that differ in final pH as a result of ammonia generation from urea hydrolysis. Acidification intervals for both strains were stochastic, despite the fact that phagolysosomes of urease deficient strains are approximately 0.5 pH units lower than those of wild type strains[15].

230

231 Trained murine macrophages have inverse acidification dynamics

232 Trained immunity has recently been shown to influence repeated infection in monocyte populations not
233 exposed to the adaptive immune system[30]. To determine whether initial exposure to a pathogen has an
234 effect in the dynamics of this system we exposed BMDMs to *C. neoformans,* resolved the infection with
235 antifungals, and measured phagolysosome acidification dynamics upon reinfection. We found that pH
236 distribution of phagolysosomes from macrophages previously trained as described also exhibited
237 stochastic behavior (Figure 6A), veering away from a normal distribution of pH (Figure 6B and SFig 8).
238 However, trained BMDMs on average exhibited a significantly lower initial pH, which became significantly
239 higher compared to untrained BMDMs over time (Figure 6C). Fully understanding this system will require
240 significant further study outside the scope of this manuscript. In this regard we note that amphotericin B
241 is a powerful activator of macrophages[31] and that *C. neoformans* residence inside macrophages is
242 associated with host cell damage[32,33]. Hence, the effects we observe could be the aggregate of several
243 influences in the system. Nevertheless, there is a clear suggestion of a historical effect on which pH
244 distribution a macrophage will employ. This may also suggest an adaptive component to the macrophage
245 bet-hedging strategy.

246

247 Differently polarized macrophages acidify stochastically but not using this bet hedging system

248 To probe whether M0 and M2 polarized macrophages acidify with the same dynamics of M1
249 macrophages, we repeated these experiments with macrophages that were either not stimulated, or
250 stimulated with IL-4 to skew towards M2. First, we found that regardless of the polarization skew all
251 macrophages acidified stochastically (Figure 7A). Second, we found that the phagolysosomal pH
252 distributions differed overall with M2 macrophages having the highest mean pH, followed by M0 and then
253 followed by M1 skewed (Figure 7B). Most striking was the observation that M0 and M2 skewed
254 macrophages did not manifest a normally distributed pH range as observed with M1 skewed
255 macrophages. Instead, M0 macrophages consistently yield a bimodal distribution even after 1 h. The M2
256 macrophages phagosomal pH distribution started with a heavy tail of higher pH and eventually stabilize
257 to a bimodal distribution. These data suggest that while the macrophages have the same underlying
258 acidification dynamics, they do not share the betting strategy of M1 skewed macrophages. Thus, we
259 estimated each population of macrophages likelihood to survive when faced with the same list of human
260 pathogens modeled after bimodal distributions estimated from the observed data (SFig 9). After
261 comparing these simulations, we found that M1 macrophages by far have the highest mean log fitness,
262 followed by M0, followed by M2 (Figure 7C). Our model shows M1 macrophages as resistant to these
263 infectious agents with M2 permissive.

264

265 Human monocytes acidify stochastically and approximate normality

266 To determine how closely the murine system resembled human acidification dynamics, we isolated
267 macrophages from human peripheral blood monocytes and repeated these experiments with beads and
268 live *C. neoformans*. We found that acidification intervals in human cells were also stochastic in nature
269 (Figure 8A). Additionally, human cells that ingested inert beads were normally distributed at the 15 min
270 and 1 h time intervals. Even though the times skewed away from normality, the skew was not as severe
271 as that observed in yeast containing phagolysosomes (Figure 8B). We hypothesize that some of this
272 skewing could result from different dynamics due to the different background inherent to human donors,
273 which differ from the mouse system in which cells are isolated from genetically identical individuals (SFig
274 10). Furthermore, within the context of our simulation, if we model the phagolysosome pH values of a
275 population of human macrophages as a normal distribution with mean and standard deviation
276 determined from pH values observed across all time points (5.08 and 1.08, respectively), the resulting
277 mean log fitness is high with dramatically reduced deviation in fitness (Figure 5).

278

279 <u>*Pathogens* skew phagolysosome acidification towards conditions less favorable to the macrophage</u>

280 Cryptococcal cells buffer the phagolysosome pH toward 5.5, a value optimal for yeast growth[14]. We
281 therefore hypothesized that *C. neoformans* could use this buffering capability to disrupt the host
282 acidification strategy. We found that phagolysosomes containing live *C. neoformans* and live *C. gattii*
283 acidified to distributions of pH less normally distributed and more permissive to general fungal replication
284 by increasing the average observed phagolysosomal pH.

285 To probe host fitness with regard to *C. neoformans* specifically, we modified our model by declaring the
286 inhibitory pH as ≤ 4, which inhibits *C. neoformans* replication[34], and calculated the likelihood of each
287 population of macrophages to achieve an inhibitory pH, assuming phagolysosome pHs were normally
288 distributed around the observed mean and standard deviation. Here we analyzed the combined data for
289 all time intervals, reasoning that in actual infection interactions between *C. neoformans* and host
290 macrophages early phagosomes would be important as well, rather than focusing only on mature
291 phagolysosomes.

292 We estimated the proportions of inhibitory phagolysosomes and found that bead-containing
293 phagolysosomes were more likely to acidify to ≤ 4, followed by heat-killed and *Δure1 C. neoformans*,
294 followed by live *C. neoformans*, with capsule deficient *Cap59* being particularly likely, and trained
295 macrophages or *C. gattii* containing phagolysosomes being particularly unlikely to achieve inhibitory pH
296 (Fig 9A). Our actual data was not normally distributed with non-bead samples though, as *C. neoformans*
297 actively modulates phagolysosomal pH. The starkest difference we observed is that, in reality, killed and
298 live *C. neoformans* phagolysosomes had the same proportion of inhibitory phagolysosomes, suggesting
299 the capsule has a more significant effect on pH modulation than we initially expected. This finding is
300 corroborated by the high proportion of inhibitory phagolysosomes in *Cap59* containing phagolysosomes,
301 a strain incapable of modulating pH since it has no capsule (Fig 9C). Additionally, the expected and
302 observed increased likelihood of bead containing phagolysosomes to inhibit *C. neoformans* replication
303 compared to live *C. neoformans* phagolysosomes was consistent between murine and human cells (Fig
304 9B,D).

305 To probe whether this phenomenon was applicable to pathogens other than *C. neoformans,* we repeated
306 this analysis with published phagolysosomal pH data from *Mycobacterium avium*[35]. We found that like *C.*
307 *neoformans,* live *M. avium* bacteria modified their resident phagolysosomal pH to be more favorable
308 toward them. In contrast, the estimated mean log fitness for the host macrophage population increased
309 when they ingested killed mycobacteria, which are unable to modulate pH (SFig 11).

310

311 **Discussion**

312 The complexity and sequential nature of the phagolysosomal maturation process combined with the
313 potential for variability at each of the maturation steps, and the noisy nature of the signaling networks
314 that regulate this process, have led to the proposal that each phagolysosome is a unique and individual
315 unit[36]. In fact, the action of kinesin and dynein motors that move phagosomes along microtubules exhibits
316 stochastic behavior, adding an additional source of randomness to the process[37]. Hence, even when the
317 ingested particle is a latex bead taken through one specific type of phagocytic receptor there is
318 considerable heterogeneity in phagolysosome composition, even within a single cell[36]. Since the
319 phagolysosome is a killing machine used to control ingested microbes, this heterogeneity implies there
320 will be differences in the microbicidal efficacy of individual phagolysosomes. This variability raises
321 fundamental questions about the nature of the dynamical system embodied in the process of phagosomal
322 maturation.

323

324 In this study, we analyzed the dynamics of phagolysosome pH variability after synchronized ingestion of
325 live yeast cells, dead yeast cells, and latex particles. We sought to characterize the acidification dynamics
326 as either stochastic—an inherently unpredictable process with identical starting conditions yielding
327 different trajectories in time, or deterministic—a theoretically predictable process with identical starting
328 conditions leading to identical trajectories. In particular, we focused our analysis on differentiating
329 stochastic vs. chaotic signatures in the trajectories of phagolysosomal pH. While both dynamics might
330 yield highly divergent trajectories for similar starting conditions (i.e. only one of 100 variables differing by
331 only a minuscule amount), a chaotic system is inherently deterministic, such that if strictly identical
332 starting conditions were replicated, the same trajectory would follow from those conditions each time. A
333 chaotic system is defined as one so sensitive to initial conditions that, in practice, initial conditions cannot
334 be replicated precisely enough to see these same trajectories followed. The dynamical signatures of such
335 systems are unique and can be differentiated from that of other deterministic or stochastic dynamics.

336

337 Irrespective of the nature of the ingested particle, we observed that the distribution of the increment of
338 phagolysosomal pH reduction was random, indicative of a stochastic process. We found no evidence that
339 phagosome acidification was a chaotic process. Systems in which a large number of variables each
340 contribute to an outcome tend to exhibit 'noise', which gives them the characteristics of a stochastic
341 dynamical system. Additionally, while particle size and shape affects ingestion time[38] the mean time to
342 ingestion for beads and *C. neoformans* particles have been shown to be 2.5 and 4.18 min, respectively[38,39].

343 Since phagocytosis was synchronized and our observations were made over a period of hours, it is unlikely
344 that the effects described here are due to noise from differences in uptake time differences. In this regard,
345 our finding that phagolysosomal pH demonstrates stochastic features is consistent with our current
346 understanding of the mechanisms involved. Quantile-Quantile (Q-Q) plots revealed that most
347 phagolysosomal pH distributions in this study manifested significant deviations from normality in several
348 instances. Specifically, this stochastic normal distribution was generated at the phagolysosomal level, as
349 evident by the fact that different phagosomes within the same macrophage manifested different pH
350 values. Hence, each macrophage contains phagolysosomes with a different pH rather than each
351 macrophage containing multiple of the same pH, such that the normal distribution observed was
352 generated at the organelle level. The most normally distributed pH sets were those resulting from the
353 ingestion of latex beads, particles that cannot modify the acidity of the phagolysosome. We note that for
354 the three *C. gattii* strains the pH distributions revealed more skewing in Q-Q plots than for the H99 *C.*
355 *neoformans* strain. Although the cause of this variation is not understood and the strain sample size is too
356 small to draw firm conclusions, we note that such variation could reflect more microbial-mediated
357 modification of the phagolysosomal pH by the *C. gattii* strains. In this regard, the capsular polysaccharide
358 of *C. gattii* strains has polysaccharide triads that are more complex[40] and, given that the cryptococcal
359 polysaccharide capsule contains glucuronic acids that can modify phagolysosomal pH via acid-base
360 properties[17], it is possible that this skewing reflects differences in phagolysosome to phagosome capsular
361 effects.

362

363 We attempted to separate the dynamics of phagolysosomal maturation from acidification by investigating
364 the accumulation of phagolysosomal maturation markers, EEA1 and V-ATPase after ingestion. Analyzing
365 the same time intervals where pH populations stabilized, namely 1 to 4 h post ingestion, we found no
366 forbidden ordinal patterns, suggesting that phagosome maturation was also a stochastic process.
367 However, the acquisition of these two maturation markers did not approximate a normal distribution at
368 any of the four time intervals, with all samples manifesting heavy right skewing. This is especially
369 interesting considering V-ATPase is responsible for pumping protons into the phagolysosome and
370 maintaining acidity. If the number of V-ATPase molecules translated directly to the number of protons
371 pumped into the phagolysosome we would expect correlation between V-ATPase staining intensity and
372 pH, and thus expect normal distributions in both. The different dynamics observed with V-ATPase
373 immunofluorescence implies the pH heterogeneity is regulated by additional mechanisms. For example,
374 it is possible that the efficacy of the V-ATPase pumps on the phagolysosomal membrane differs from pump
375 to pump and that these differences also contribute to the distribution of phagolysosomal pHs observed.

376

377 For most microbes, maintenance of an acidic environment in the phagolysosome is critically determinant
378 on the integrity of the phagolysosomal membrane, keeping protons in the phagolysosomal lumen whilst
379 excluding more alkaline cytoplasmic contents. For example, with *C. albicans,* the rupture of the
380 phagolysosomal membrane is followed by rapid alkalization of the phagolysosomal lumen[41]. For *C.*
381 *neoformans*, phagolysosomal integrity is compromised by secretion of phospholipases that damage
382 membranes as well as the physical stress on membranes resulting from capsular enlargement in the

383 phagolysosome[14]. However, for *C. neoformans*, loss of phagolysosomal membrane integrity does not
384 immediately result in loss of phagolysosomal acidity, which is attributed to buffering by glucuronic acid
385 residues in the *C. neoformans* capsule[17]. Adding to the complexity of the *C. neoformans*-macrophage
386 interaction is the fact that the phagolysosomal pH in the vicinity of 5.5 matches the optimal replication
387 pH for this fungus[15], which can be expected to place additional stress on the organelle membrane through
388 the increased volume resulting from budding cells. Treating macrophages with chloroquine, which
389 increases phagosomal pH[42], potentiates macrophage antifungal activity against *C. neoformans*[43]. Hence,
390 phagosomal acidification does not inhibit *C. neoformans* replication but is critical for activation of
391 mechanisms involved in antigen presentation[44]. In the cryptococcal-containing phagolysosome the
392 luminal pH is also likely to reflect a variety of microbial-mediated variables which include ammonia
393 generation from urease, capsular composition, and the integrity of the phagolysosomal membrane.

394

395 Analysis of the normality of phagolysosomal pH distributions as a function of time by the Shapiro-Wilk
396 test produced additional insights into the dynamics of these systems. Phagolysosomes containing inert
397 beads manifested pH distributions that met criteria for normality at most time intervals after 1 h post
398 infection (HPI). We hypothesize that at 0.25 and 0.5 HPI there are two populations of phagolysosomes,
399 mature and maturing, with the latter having not yet fully acidified and thus resulting in the observed
400 bimodal distributions. Additionally, it has been shown that phagolysosomes of macrophages undergo
401 active alkalization, regulated in part by NOX2 activity[45–47]. It is likely that these early time points veer away
402 from normality due to a combination of phagolysosomes maturing at a different rate and a subpopulation
403 of phagolysosomes which are actively alkalized, both contributing noise to early phagolysosomal
404 dynamics. In contrast, the pH distribution of phagolysosomes containing dead *C. neoformans* cells initially
405 veered away from normality at 15 min, 30 min, and 1 h but in later time intervals approached normality,
406 meeting the criteria for normality at 3 h. One interpretation of this result is that the process of
407 phagocytosis is itself a randomizing system with Gaussian noise resulting from phagolysosome formation
408 and kinetics of the initial acid-base reactions between increasing proton flux and quenching glucuronic
409 acids in the capsular polysaccharide. With time, the titration is completed as all glucuronic acid residues
410 are protonated, as dead cells did not synthesize additional polysaccharide, which moved the
411 phagolysosomal pH distribution towards normality. A similar effect may have occurred with strains R265,
412 W179, and *ure1Δ*. Convergence to or away from normality could reflect a myriad of such variables
413 affecting phagolysosomal pH including the intensity of acidification, the volume of the phagolysosome
414 (largely determined by the yeast capsule radius), the glucuronic acid composition of the capsule, the
415 production of ammonia by urease, and the leakiness of the phagolysosome to cytoplasmic contents with
416 higher pH. Although our experiments cannot sort out the individual contributions of these factors, they
417 suggest that, in combination, they produce Gaussian noise effects that push or pull the resulting
418 distribution to or from normality. Additionally, human phagolysosome acidification dynamics resembled
419 those of mouse cells but noted significant differences in the distributions of phagolysosomal pH between
420 individual human donors. This donor-to-donor variation could reflect differences in polymorphisms in Fc
421 receptor genes or other genetic variables and is an interesting subject for future studies.

422

423 When a phagocytic cell ingests a microbe, it has no information as to the pH range tolerated by the
424 internalized microbe. A stochastic dynamical process for phagolysosomal acidification could provide
425 phagocytic immune cells and their hosts with the best chance for controlling ingested microbes. The acidic
426 pH in the phagolysosome activates microbicidal mechanisms and acidity is not generally considered a
427 major antimicrobial mechanism in itself. However, our analysis of pH tolerances of 27 pathogenic
428 microbes revealed that the majority are inhibited by phagolysosomal pH with the caveat that some, like
429 *C. neoformans*[18] and *Salmonella typhimrium*[48], thrive in acidified phagolysosomes. On the other hand, a
430 less acidic phagosomal pH is conducive to intracellular survival for *M. tuberculosis*[49]. During an infectious
431 process when the immune system confronts numerous microbial cells the random nature of the final
432 phagosomal pH will result in some fraction of the infecting inoculum being controlled, and possibly killed,
433 by initial ingestion allowing antigen presentation. In this regard, the mean number of bacteria in the
434 phagolysosomes and cytoplasm of macrophages infected with the intracellular pathogen *Franciscella*
435 *tularensis* exhibits stochastic dynamics[50], which in turn could result from the type of stochastic processes
436 in phagolysosome formation noted here. Hence, chance in phagolysosomal pH acidification provides
437 phagocytic cells with a mechanism to hedge their bets such that the stochastic nature of the process is
438 itself a host defense mechanism.

439

440 In biology, bet-hedging was described by Darwin as a strategy to overcome an unpredictable
441 environment[51], which is now known as diversified bet-hedging: diversifying offspring genotype to ensure
442 survival of at least some individuals at the expense of reducing the mean inclusive fitness of the parent.
443 The main idea behind any bet-hedging strategy, under the assumption of multiplicative fitness, is that to
444 maximize long-term fitness, an organism must lower its variance in fitness between generations[52–54]. For
445 example, varying egg size and number in a clutch can bank against years with a hostile environment in a
446 form of diversified bet-hedging[55]. During any given "good year" fewer of the offspring will thrive because
447 some are specifically designated for survival in "bad years", drastically increasing fitness during bad years
448 at the cost of a slight fitness reduction during good. Our observations suggest that, as a population,
449 macrophages perform a bet-hedging strategy by introducing a pH level as inhospitable to pathogens as
450 possible, while still maintaining biologically possible levels. However, such an approach could select for
451 acid-resistant microbes. Our observation suggests that to avoid an arms-race, the macrophage not only
452 lowers the pH level to a level that is unfavorable to most microbes, since the reduction in pH level reduces
453 the optimal growth condition to around 70% of the optimum (see Figure 3 red line under the blue shaded
454 curve), but it also introduces randomness in the achieved pH, such that ingested microbes are less likely
455 to adapt to the potentially hostile environment. In other words, tightly controlled pH reduction by the
456 host without increased variation, might introduce an evolutionary arm-race between pathogens and their
457 host cells, leading towards deleterious outcome of selecting microbial acid resistance. A similar
458 evolutionary arms race would occur between environmental *C. neoformans* and the amoebas who prey
459 upon them. Previous studies indicate that acidification in amoebas closely resembles that of macrophages
460 with similar final pH and time to acidification[56,57]. Thus, phagocytic predators in soils would face the same
461 problem as macrophages in not knowing the pH tolerance of their prey and it is conceivable that they
462 employ a similar defense strategy to that observed in macrophages, likely to have been honed in by eons
463 of selection in soil predator-prey interactions.

464

465 Additionally, our model shows that even at the lower extreme mean pH, macrophage populations still
466 benefit in the long run by increasing their phagolysosomal pH variance. We note that the pH of other
467 mammalian fluids such as that of the blood are tightly regulated such that their physiological variance is
468 very small[58]. For example, human plasma pH averages 7.4 with a range of only 0.05 units. Hence,
469 organisms can maintain tight pH control when it is physiologically important, implying that the
470 comparatively large range of phagolysosomal pHs measured in all conditions studied is a designed feature
471 of this system. In other words, one can envision the macrophage's first line of defense of bet-hedging
472 phagolysosomal pH as a roulette wheel, where the payout is likelihood of macrophage survival and the
473 placed bet is a range of possible pH. Placing multiple bets across the table (increasing standard deviation
474 of pH distribution) increases the chance of winning at the cost of a lower payout (mean fitness), resulting
475 in a more profitable long-term strategy (increased mean log fitness). In fact, the most profitable roulette
476 strategy is broad color bets with lower payouts but the best winning probability. The most profitable
477 betting strategy would of course be to play Blackjack instead, but macrophages do not have that luxury.

478

479 We observed that this bet hedging strategy was displayed in M1 polarized macrophages, dependent on a
480 normal distribution of phagolysosomal pH with a high variance. M2 macrophages, which acidify with
481 different dynamics to M1[59], do not acidify to a normal distribution and thus do not engage in this bet
482 hedging strategy. Additionally, we found that M2 skewed macrophage populations on average acidify to
483 a higher pH than M1 skewed populations and are overall more favorable to *C. neoformans*, an observation
484 supported by previous literature[59,60]. This hypothesis, while requiring more investigation, may help explain
485 why M2 skewed macrophages are unable to control *C. neoformans* infection, as their phagolysosomes
486 acidify to a pH range that is optimal for *C. neoformans* growth[15].

487

488 Additionally, intracellular pathogens have developed their own ways to disrupt or game the macrophage
489 betting system. For *C. neoformans*, which can manipulate phagolysosomal pH through several
490 mechanisms, our model shows that the fungal-mediated changes in the distribution of phagolysosomal
491 pH favors the pathogen overall, disrupting the bet hedging system and resulting in lower macrophage
492 population fitness. This phenomenon can also be observed with *M. avium* in which previously reported
493 phagolysosomal pH values[35] show a marked increase in mean log fitness when the ingested pathogen is
494 killed and unable to modulate pH. This finding is emphasized by our analysis of phagolysosomes whose
495 pH has been pharmacologically manipulated to a region favorable to pathogens. We found that disrupting
496 the macrophage betting system this way led to a drastically reduced overall mean log fitness of the
497 macrophage population.

498

499 Given that acid has potent antimicrobial properties, one might wonder why phagolysosomal acidification
500 does not reach even lower and more acidic pHs. There are several explanations for observed lower limits
501 in pH. Acidification is achieved by pumping protons into the vacuole and achieving lower pHs against an

502 ever-increasing acidity gradient could prove thermodynamically difficult. There is also evidence that the
503 integrity of the cell membrane lipid bilayer is compromised by acidity at pHs of 3 and below[61,62] which
504 could promote leakage of phagolysosomal contents into the cytoplasm with damage to the host cell.
505 Consequently, we propose that a larger variation in macrophage phagolysosomal pH acts as a diversified
506 bet-hedging strategy against the stochasticity of the potential pH tolerances of ingested microbes within
507 the physiological limits of achievable acidification. This hypothesis is supported by simulated data in which
508 an increase in standard deviation of the pH distribution slightly lowers the expected mean but significantly
509 decreases the standard deviation of host survival. Fully analyzing the consequences and evolutionary
510 tradeoff of this strategy would require a closer analysis that considers the costs and benefits with regard
511 to the host. Though outside the scope of our current work, our observations suggest this line of
512 investigation for future studies.

513

514 Our results delineate new avenues for investigation. Most perplexing is how a random phagolysosomal
515 pH is established and maintained. One can imagine various mechanisms including variation in the number
516 of ATPase molecules and/or differences in activity of individual pumps depending on location and
517 adjoining structures. To resolve this would require sophisticated technology allowing the measurement
518 of pH in individual phagolysosomes as a function of pump occupancy and efficacy. Such techniques are
519 likely beyond the current technological horizon but suggests new fertile areas of scientific investigation.
520 From a clinical perspective, a drug that increases variation in phagolysosomal pH could be useful in
521 enhancing macrophage anti-microbial efficacy in situations that one cannot anticipate which specific
522 microbes will be encountered. On the other hand, drugs that specifically modulate pH may be useful in
523 situations with specific microbes that express marked acid/base tolerance. In this regard, chloroquine
524 alkalizes *C. neoformans* phagolysosomes, moving away from optimal inhibitory pH. This drug has been
525 shown to enhance macrophage activity against *C. neoformans*[9,63], an outcome predicted by our model.

526

527 In summary, we document that phagolysosomal acidification, a critical process for phagocytic cell efficacy
528 in controlling ingested microbial cells, manifests stochastic dynamics that permit a bet-hedging strategy
529 for phagocytic cells ingesting microbes of unknown pH tolerance. These observations establish that the
530 use of bet-hedging strategies in biology extends to the sub-organism level to involve cells and their
531 organelles. This, in turn, implies a significant role for chance in the resolution of conflict between microbes
532 and host phagocytic cells in individual phagolysosomes. We have recently argued that chance is also a
533 major determinant of individual susceptibility to infectious diseases at the organismal level[64]. Variability
534 in the outcome of infectious disease between individual hosts may reflect the sum of innumerable chance
535 events for host-microbe interactions at the cellular level, which include the process of phagosome
536 acidification.

537

538 **Methods**

539 <u>Cell Strains and Culture Conditions</u>

540 *Cryptococcus gattii* species complex strains R265, WM179, and WM161 were obtained from ATCC
541 (Manassas, VA), and *Cryptococcus neoformans* species complex serotype A strain H99 as well as *ure1Δ*
542 (lacking urease, derived from H99) were originally obtained from John Perfect (Durham, NC). The strains
543 were stored at 80°C.Frozen stocks were streaked onto Sabouraud dextrose agar (SAB) and incubated at
544 30°C. Liquid suspensions of cryptococcal cultures were grown in SAB overnight at 30°C. Cryptococcal
545 cultures were heat killed by incubating at 65 °C for 1 h.

546 Macrophage cells were either mouse bone marrow-derived macrophages (BMDM) obtained from 6 week
547 old C57BL/6 female mice from The Jackson Laboratory (Bar Harbor, ME), J774.16 macrophage-like cells,
548 or human monocytes isolated from PMBCs. BMDMs were isolated from hind leg bones and for
549 differentiation were seeded in 10 cm tissue culture treated dishes (Corning, NY) in Dulbecco's Modified
550 Eagle Medium (DMEM, Corning) with 10% FBS (Atlanta Biologicals, Flowery Branch, GA), 1% nonessential
551 amino acids (Cellgro, Manassas, VA), 1% penicillin-streptomycin (Corning), 2 mM Glutamax (Gibco,
552 Gaithersburg, MD), 1% HEPES buffer (Corning), 20% L-929 cell conditioned supernatant, 0.1% beta-
553 mercaptoethanol (Gibco) for 6 days at 37 °C and 9.5% CO_2. BMDMs were used for experiments within 5
554 days after differentiation. J774.16 cells were cultured in DMEM with 10% FBS, 1% nonessential amino
555 acids, 10% NCTC109 (Gibco), and 1% penicillin-streptomycin at 37 °C with 9.5% CO_2. For human peripheral
556 blood mononuclear cells (hPBMCs), CD14+ monocytes were isolated using Dynabeads Untouched Human
557 Monocytes Kit (Thermo Fisher Scientific) according to the manufacturer protocol. The isolated cells were
558 differentiated in RPMI-1640 medium (RPMI) with 10% FBS (Atlanta Biologicals, Flowery Branch, GA), 1%
559 penicillin-streptomycin (Corning), and 25 ng/mL of human granulocyte-macrophage colony-stimulating
560 factor (GM-CSF, Sigma-Aldrich) for five days. Human cells were further cultured in RPMI (RPMI) with 10%
561 FBS (Atlanta Biologicals, Flowery Branch, GA), 1% penicillin-streptomycin (Corning), and activated with 0.5
562 ug/mL lipopolysaccharide (LPS; Sigma-Aldrich) and 10 ng/mL interferon gamma (IFN-γ; Roche) for M1
563 polarization or 20 ng/mL IL-4 for M2 polarization.

564

565 <u>Phagolysosomal pH measurement</u>

566 Phagolysosomal pH was measured using ratiometric fluorescence imaging involving the use of pH-
567 sensitive probe Oregon green 488 as described in prior studies[15]. The pH values analyzed here were
568 collected in part during prior studies of *C. neoformans*-macrophage interactions[14–16]. Briefly, Oregon green
569 488 was first conjugated to monoclonal antibody (mAb) 18B7, which binds *C. neoformans* capsular
570 polysaccharide, using Oregon Green 488 Protein Labeling Kit (Molecular Probes, Eugene, OR). The labeling
571 procedure was done by following the manufacture's instruction. BMDMs were plated at a density of 1.25
572 × 10^5 cells/well or differentiated human macrophages were plated at a density of 2.5 x 10^5 cells/well on
573 24-well plate with 12 mm circular coverslip. Cells were activated with 0.5 µg/ml LPS and 100 U/ml IFN-γ
574 or 20 ng/mL IL-4 as previously described at 37 °C in a 9.5% CO_2 (BMDM) or 5% CO_2 (Human macrophage)
575 atmosphere overnight. Prior to infection, 2 d old live, heat killed H99, R265, WM179, ure1, cap59, or anti-
576 mouse IgG coated polystyrene bead (3.75 × 10^6 cells or beads/ml) were incubated with 10 µg/ml Oregon
577 green conjugated mAb 18B7 for 15 min. Macrophages were then incubated with Oregon green conjugated
578 mAb 18B7-opsonized particles in 3.75 × 10^5 cryptococcal cells or beads per well (BMDM) or 2.5 x 10^5
579 cell/well (Human macrophage). For drug treatment experiments the macrophage cell media was

580 supplemented with 3 µM chloroquine. Cells were either centrifuged immediately at 350 x g for 1 min or
581 incubated at 4 °C for 30 min to synchronize ingestion and cultures were incubated at 37 °C for 10 min to
582 allow phagocytosis. Extracellular cryptococcal cells or beads were removed by washing three times with
583 fresh medium, a step that prevents the occurrence of new phagocytic events. As an additional safeguard
584 against new phagocytic events fresh media was supplemented with AlexaFluor 568 conjugated mAb 18B7
585 for 1 h to label extracellular particles. Samples on coverslip were collected at their respective time points
586 after phagocytosis by washing twice with pre-warmed HBSS and placing upside down on MatTek petri
587 dish (MatTek, Ashland, MA) with HBSS in the microwell. Images were taken by using Olympus AX70
588 microscopy (Olympus, Center Valley, PA) with objective 40x at dual excitation 440 nm and 488 nm, and
589 emission 520 nm. Images were analyzed using MetaFluor Fluorescence Ratio Imaging Software (Molecular
590 Devices, Downingtown, PA). Fluorescence intensities were used to determine the ratios of Ex488
591 nm/Ex440 nm that were converted to absolute pH values using a standard curve where the images are
592 taken as above but intracellular pH of macrophages was equilibrated by adding 10 µM nigericin in pH
593 buffer (140 mM KCl, 1 mM $MgCl_2$, 1 mM $CaCl_2$, 5 mM glucose, and appropriate buffer ≤ pH 5.0: acetate-
594 acetic acid; pH 5.5-6.5: MES; ≥ pH 7.0: HEPES. Desired pH values were adjusted using either 1 M KOH or 1
595 M HCl). The pH of buffers was adjusted at 3-7 using 0.5-pH unit increments.

596

597 Immunofluorescence Microscopy

598 BMDMs were seeded on 12 mm circular coverslips in 24 well tissue culture plates at 2.5 * 10^5 cells per
599 well. Cells were activated with 0.5 µg/ml lipopolysaccharide and 100 U/ml interferon gamma at 37 °C in a
600 9.5% CO_2 atmosphere overnight. Anti-mouse IgG coated beads were opsonized with 10 µg/mL and added
601 to cells at MOI 1. Phagocytosis was synchronized by centrifuging the plate at 350 x g for 1 min before
602 being incubated at 37 °C. At each timepoint media was replaced with 4% paraformaldehyde (PFA) and
603 incubated for 10 min at room temperature to fix cells. PFA was removed and cells were washed three
604 times with 1 mL PBS (1X). Coverslips were blocked for 1 h at room temperature with 2% BSA in PBS.
605 Primary incubation was performed with Rb αEEA1 (ThermoFisher Scientific MA5-14794) at 1:100 dilution
606 or Rb αV-ATPase (ThermoFisher Scientific PA5-29899) at 1:100 dilution in blocking buffer for 1 h at room
607 temperature. Coverslips were washed with blocking buffer before secondary incubation with Goat αRb
608 AlexaFluor 488 (1:100) in blocking buffer for 1 h at room temperature. Coverslips were washed once more
609 with dH_2O and mounted on glass slides using Prolong Gold mounting agent. Slides were imaged via Zeiss
610 Axiovert 200M microscope and intensity was analyzed using Zeiss Lite Blue Version. A region of interest
611 was generated by outlining the ingested bead via phase contrast channel then measuring mean
612 fluorescence intensity of the secondary antibody.

613

614 Trained macrophage experiments

615 BMDMs were plated at a density of 2 × 10^5 cells/well on 24-well plate with 12 mm circular coverslip.
616 Cells were activated with 0.5 µg/ml LPS and 100 U/ml IFN-γ; Roche and incubated at 37 °C in a 9.5% CO_2
617 atmosphere overnight. Prior to the infection, H99 were stained with 0.01% Uvitex 2B for 10 min.
618 BMDMs were then infected with H99 (2 × 10^5 cells/well) in the presence of 10 µg/ml 18B7. After 1 h of

619 infection, 5 µg/ml of amphotericin B were added to each well and the culture were incubated for
620 overnight. On the following day, the cultures were washed three times with PBS, and incubated in PBS
621 for 2 h. After the incubation, the cultures were further washed three times with PBS. A fresh overnight
622 culture of H99 were incubated with 10 µg/ml Oregon green conjugated mAb 18B7 for 15 min.
623 Macrophages were then incubated with Oregon green conjugated mAb 18B7-opsonized H99 in 2×10^5
624 cells per well. Cells were centrifuged immediately at 350 x g for 1 min to synchronize ingestion.
625 Phagolysosomal pH were then measured using Olympus AX70 microscopy.

626

627 Time-lapse imaging and intracellular replication

628 The time of intracellular replication here were collected in time-lapse imaging during prior studies of *C.*
629 *neoformans*-macrophage interactions[15]. For imaging BMDM (5×10^4 cells/well) were plated on poly-D-
630 lysine coated coverslip bottom MatTek petri dishes with 14mm microwell (MatTek). Cells were cultured
631 in completed DMEM medium and stimulated with 0.5 µg/ml LPS and 100 U/ml IFN-γ overnight at 37 °C
632 with 9.5 % CO_2. On the following day, macrophages were infected with cryptococcal cells (H99 or ure1;
633 1.5×10^5 cells/well) opsonized with 18B7 (10 µg/ml). After 2 h incubation to allow phagocytosis,
634 extracellular cryptococcal cells were removed by washing the culture five times with fresh medium.
635 Images were taken every 4 min for 24 h using a Zeiss Axiovert 200M inverted microscope with a 10x phase
636 objective in an enclosed chamber at 9.5 % CO_2 and 37 °C. The time intervals to initial replication of
637 individual cryptococcal cells inside macrophage were measured in time-lapse imaging.

638

639 Data Processing

640 Phagolysosome pH intervals were calculated by subtracting measured pH levels of phagolysosomes from
641 a starting pH of 7.2, the pH of the surrounding media, and individual interval measurements were
642 concatenated into a single dataset for each time point examined.

643

644 Data analysis

645 Discrimination of deterministic vs. stochastic dynamics was achieved using the previously characterized
646 permutation spectrum test[21]. In this method, the processed datasets were segmented into overlapping
647 subsets of 4 data points using a sliding window approach, as detailed in figure 4, and assigned 1 of 24 (4!)
648 possible ordinal patterns based on the ordering of the 4 terms in the subset. The frequencies with which
649 each unique ordinal pattern occurred in the dataset were then calculated and plotted. Deterministic
650 dynamics were characterized by the occurrence of "forbidden ordinals", equal to ordinal patterns that
651 doesn't occur in the dataset whereas stochastic dynamics were characterized by the presence of all
652 ordinals. Measured phagolysosomal pHs were subtracted from an initial pH value (7.2) based on cell media
653 pH and placed in a vector. Subsets of 4 data points were generated using a sliding window approach in
654 which the first four values were grouped, the window shifted by one, and the subsequent set of 4 values
655 grouped. Each subset was prescribed an "ordinal pattern" based on the relative values of the data points

in the subset to each other with, for instance, the lowest value assigned a "0" in the ordinal pattern and the highest a "3". Further characterization of deterministic dynamics was achieved using the previously characterized point count plot[65], in which periodic vs. chaotic dynamics were differentiated based on the distribution of "peaks" in the calculated power spectrum of each dataset. Power spectrums were estimated with Matlab's Lomb-Scargle power spectral density (PSD) estimate function and subsequently normalized. From the normalized power spectrum, "point count plots" were generated by counting the number of peaks above a set threshold—the point threshold—with values of the point threshold ranging from 0 to 1. Periodic dynamics were characterized by "staircase" point count plots whereas chaotic dynamics were characterized by point count plots with a decreasing exponential shape.

Distribution and normality analysis

Each set of sample data was fit to a series of distributions using the R package "fitdistrplus" with default parameters for each distribution type, generating the histograms and Quantile-Quantile (Q-Q) plots. Normality and significance were calculated via the base R Shapiro-Wilk test.

Generating and Analyzing Simulations

Let f(x) be the probability distribution of the host's pH. For simplicity, we assume that f is Normal(μ, σ). Let F(x) be the corresponding cdf. At every time-point, we randomly sample a pathogen i from a set of pathogens. The pathogen has a range (a_i,b_i) of viable pH, which differs among pathogens. Minimum tolerable pH values were obtained from the literature as described, while a constant value of 8 was used for maximum since most pathogens were inhibited as high pH as well as phagolysosomes being unlikely to alkalize. The host, in turn, randomly chooses a pH by sampling from the distribution f(x). If the host's pH x falls in the interval (a_i,b_i), then there is a probability p of the host dying. We can think of the host's survival rate ρ as its fitness, which is a random variable that depends on the randomness in pathogens. As a function of i, we have ρ(i)=p*(F(b_i)-F(a_i)); the random variable ρ assumes the values ρ(i) with equal probability. Additionally, since biologically relevant phagolysosome pH values will only fall within a certain range, we decided to limit the possible pH values between 2 and 7.2 (pH of associated cell media). Any values generated outside those limits were instead recorded as their respective limit. Thus, distributions become less normally distributed at the extremes, sacrificing normality for biological practicality, as real phagolysosomes would not alkalize or be likely to acidify below 2. In these situations, we calculated outputs based on 1,000 replicates of 10,000 simulated phagolysosomes each.

Author Contributions

Conceptualization, Q.D., K.S., A.V, A.C; Methodology: Q.D., K.S., Y.S., M.F., Y.S., C.Y., A.B., A.C.; Software, Q.D., K.S., Y.S., A.V.; Formal Analysis, Q.D.; Investigation, Q.D., K.S., Y.S., M.F., Y.S., C.Y., I.Y., C.M.DLR, J.F., A.B., A.C.; Writing – Original Draft, Q.D., K.S., M.F, A.B., A.C.; Writing – Review & Editing, Q.D., K.S., Y.S., M.F., Y.S., C.Y., I.Y., C.M.DLR, J.F., A.B., A.C.; Visualization, Q.D.

Acknowledgements

Arturo Casadevall was supported by grants R01HL059842, 5R01AI033774, 5R37AI033142, and 5R01AI052733. Quigly Dragotakes is supported by a fellowship from the Achievement Rewards for College Scientists (ARCS) Foundation Metro-Washington Chapter as well as a National Institutes of Health T32.

References

1. Broderick, N. A. A common origin for immunity and digestion. *Front Immunol* **6**, 72 (2015). [PMID:25745424]

2. Rosales, C.; Uribe-Querol, E. Phagocytosis: A Fundamental Process in Immunity. *Biomed Res Int* **2017**, 9042851 (2017). [PMID:28691037]

3. Sun-Wada, G. H.; Tabata, H.; Kawamura, N.; Aoyama, M.; Wada, Y. Direct recruitment of H+-ATPase from lysosomes for phagosomal acidification. *J Cell Sci* **122**, 2504–2513 (2009). [PMID:19549681]

4. Kinchen, J. M.; Ravichandran, K. S. Phagosome maturation: going through the acid test. *Nat Rev Mol Cell Biol* **9**, 781–795 (2008). [PMID:18813294]

5. Jankowski, A.; Scott, C. C.; Grinstein, S. Determinants of the phagosomal pH in neutrophils. *J Biol Chem* **277**, 6059–6066 (2002). [PMID:11744729]

6. Bouvier, G.; Benoliel, A. M.; Foa, C.; Bongrand, P. Relationship between phagosome acidification, phagosome-lysosome fusion, and mechanism of particle ingestion. *J Leukoc Biol* **55**, 729–734 (1994). [PMID:8195699]

7. Geisow, M. J.; D'Arcy Hart, P.; Young, M. R. Temporal changes of lysosome and phagosome pH during phagolysosome formation in macrophages: studies by fluorescence spectroscopy. *J Cell Biol* **89**, 645–652 (1981). [PMID:6166620]

8. Feldmesser, M.; Kress, Y.; Novikoff, P.; Casadevall, A. Cryptococcus neoformans is a facultative intracellular pathogen in murine pulmonary infection. *Infection and Immunity* **68**, 4225–4237 (2000).

9. Levitz, S. M.; Nong, S. H.; Seetoo, K. F.; Harrison, T. S.; Speizer, R. A.; Simons, E. R. Cryptococcus neoformans resides in an acidic phagolysosome of human macrophages. *Infection and Immunity* **67**, 885–890 (1999).

10. Ma, H.; Croudace, J. E.; Lammas, D. A.; May, R. C. Expulsion of Live Pathogenic Yeast by Macrophages. *Current Biology* **16**, 2156–2160 (2006). [PMID:17084701]

11. Alvarez, M.; Casadevall, A. Phagosome fusion and extrusion, and host cell survival following Cryptococcus neoformans phagocytosis by macrophages. *Current Biology* **16**, 2161–2165 (2006).

12. Ma, H.; Croudace, J. E.; Lammas, D. A.; May, R. C. Direct cell-to-cell spread of a pathogenic yeast. *BMC immunology* **8**, 15 (2007). [PMID:17705831]

13. Alvarez, M.; Casadevall, A. Cell-to-cell spread and massive vacuole formation after Cryptococcus

730 neoformans infection of murine macrophages. *BMC immunology* **8**, 16 (2007).

731 **14**. De Leon-Rodriguez, C. M.; Rossi, D. C. P.; Fu, M. S.; Dragotakes, Q.; Coelho, C.; Guerrero Ros, I.;
732 Caballero, B.; Nolan, S. J.; Casadevall, A. The Outcome of the *Cryptococcus neoformans*–
733 Macrophage Interaction Depends on Phagolysosomal Membrane Integrity. *The Journal of*
734 *Immunology* **201**, 583–603 (2018).

735 **15**. Fu, M. S.; Coelho, C.; De Leon-Rodriguez, C. M.; Rossi, D. C. P.; Camacho, E.; Jung, E. H.; Kulkarni,
736 M.; Casadevall, A. Cryptococcus neoformans urease affects the outcome of intracellular
737 pathogenesis by modulating phagolysosomal pH. *PLOS Pathogens* **14**, e1007144 (2018).

738 **16**. Freij, J. B.; Fu, M. S.; De Leon Rodriguez, C. M.; Dziedzic, A.; Jedlicka, A. E.; Dragotakes, Q.; Rossi,
739 D. C. P.; Jung, E. H.; Coelho, C.; Casadevall, A. Conservation of Intracellular Pathogenic Strategy
740 among Distantly Related Cryptococcal Species. *Infection and Immunity* **86**, (2018).

741 **17**. De Leon-Rodriguez, C. M.; Fu, M. S.; Corbali, M. O.; Cordero, R. J. B.; Casadevall, A. The Capsule of
742 Cryptococcus neoformans Modulates Phagosomal pH through Its Acid-Base Properties. *mSphere*
743 **3**, (2018). [PMID:30355667]

744 **18**. DeLeon-Rodriguez, C. M.; Casadevall, A. Cryptococcus neoformans: Tripping on Acid in the
745 Phagolysosome. *Frontiers in Microbiology* **7**, 164 (2016).

746 **19**. Smith, L. M.; Dixon, E. F.; May, R. C. The fungal pathogen *C ryptococcus neoformans* manipulates
747 macrophage phagosome maturation. *Cellular Microbiology* **17**, 702–713 (2015).
748 [PMID:25394938]

749 **20**. Davis, M. J.; Eastman, A. J.; Qiu, Y.; Gregorka, B.; Kozel, T. R.; Osterholzer, J. J.; Curtis, J. L.;
750 Swanson, J. A.; Olszewski, M. A. Cryptococcus neoformans-induced macrophage lysosome
751 damage crucially contributes to fungal virulence. *J Immunol* **194**, 2219–2231 (2015).
752 [PMID:25637026]

753 **21**. Zunino, L.; Soriano, M. C.; Rosso, O. A. Distinguishing chaotic and stochastic dynamics from time
754 series by using a multiscale symbolic approach. *Phys. Rev. E. Stat. Nonlin. Soft. Matter Phys* **86**,
755 46210 (2012).

756 **22**. McCullough, M.; Sakellariou, K.; Stemler, T.; Small, M. Counting forbidden patterns in irregularly
757 sampled time series. I. The effects of under-sampling, random depletion, and timing jitter. *Chaos*
758 **26**, 123103 (2016).

759 **23**. Sakellariou, K.; McCullough, M.; Stemler, T.; Small, M. Counting forbidden patterns in irregularly
760 sampled time series. ii. reliability in the presence of highly irregular sampling. *Chaos* **26**, 123104
761 (2016).

762 **24**. Rosso, O. A.; Carpi, L. C.; Saco, P. M.; Ravetti, M. G.; Larrondo, H. A.; Plastino, A. Noisy-chaotic
763 time series and the forbidden/missing patterns paradigm. (2011).

764 **25**. Skiadas, C. H.; Skiadas, C. *Handbook of applications of chaos theory*

765 **26**. Fierer, N.; Jackson, R. B. The diversity and biogeography of soil bacterial communities. *Proc Natl*
766 *Acad Sci U S A* **103**, 626–631 (2006). [PMID:16407148]

767 **27**. Baath K., E. ;Arnebrand. Growth rate and response of bacterial communities to pH in limed and
768 ash treated forest soils. *Soil Biol. Biochem.* **26**, 995–1001 (1994).

769 **28**. Baath, E.; Frostegard, A.; Fritze, H. Soil Bacterial Biomass, Activity, Phospholipid Fatty Acid
770 Pattern, and pH Tolerance in an Area Polluted with Alkaline Dust Deposition. *Appl Environ*
771 *Microbiol* **58**, 4026–4031 (1992). [PMID:16348828]

772 **29**. Karlin, S.; Lieberman, U. Random temporal variation in selection intensities: case of large
773 population size. *Theoretical population biology* **6**, 355–382 (1974). [PMID:4460262]

774 **30**. Quintin, J.; Saeed, S.; Martens, J. H. A.; Giamarellos-Bourboulis, E. J.; Ifrim, D. C.; Logie, C.; Jacobs,
775 L.; Jansen, T.; Kullberg, B.-J.; Wijmenga, C.; Joosten, L. A. B.; Xavier, R. J.; van der Meer, J. W. M.;
776 Stunnenberg, H. G.; Netea, M. G. Candida albicans infection affords protection against reinfection
777 via functional reprogramming of monocytes. *Cell host & microbe* **12**, 223–232 (2012).
778 [PMID:22901542]

779 **31**. Sau, K.; Mambula, S. S.; Latz, E.; Henneke, P.; Golenbock, D. T.; Levitz, S. M. The Antifungal Drug
780 Amphotericin B Promotes Inflammatory Cytokine Release by a Toll-like Receptor- and CD14-
781 dependent Mechanism. *Journal of Biological Chemistry* **278**, 37561–37568 (2003).
782 [PMID:12860979]

783 **32**. Casadevall, A.; Coelho, C.; Alanio, A. Mechanisms of Cryptococcus neoformans-Mediated Host
784 Damage. *Front Immunol* **9**, 855 (2018). [PMID:29760698]

785 **33**. Coelho, C.; Souza, A. C. O.; Derengowski, L. da S.; de Leon-Rodriguez, C.; Wang, B.; Leon-Rivera,
786 R.; Bocca, A. L.; Gonçalves, T.; Casadevall, A. Macrophage mitochondrial and stress response to
787 ingestion of Cryptococcus neoformans. *Journal of Immunology (Baltimore, Md.: 1950)* **194**, 2345–
788 2357 (2015).

789 **34**. Alspaugh, J. A.; Granger, D. L. Inhibition of Cryptococcus neoformans replication by nitrogen
790 oxide supports the role of these molecules as effectors of macrophage-mediated cystostasis.
791 *Infect. Immun* **59**, 2291–2296 (1991).

792 **35**. Oh, Y. K.; Straubinger, R. M. Intracellular fate of Mycobacterium avium: use of dual-label
793 spectrofluorometry to investigate the influence of bacterial viability and opsonization on
794 phagosomal pH and phagosome-lysosome interaction. *Infect Immun* **64**, 319–325 (1996).
795 [PMID:8557358]

796 **36**. Griffiths, G. On phagosome individuality and membrane signalling networks. *Trends Cell Biol* **14**,
797 343–351 (2004). [PMID:15246427]

798 **37**. Mallik, K. C. B.; Banerjee, P. L.; Chatterjee, B. D.; Pramanick, M. An experimental study of the
799 course of infection in mice after intranasal insufflation with Cryptococcus neoformans. *Ind. J.*
800 *Med. Res* **54**, 608–610 (1966).

801 **38**. Paul, D.; Achouri, S.; Yoon, Y.-Z.; Herre, J.; Bryant, C. E.; Cicuta, P. Phagocytosis dynamics depends
802 on target shape. *Biophysical journal* **105**, 1143–1150 (2013). [PMID:24010657]

803 **39**. Dragotakes, Q.; Fu, M. S.; Casadevall, A. Dragotcytosis: Elucidation of the Mechanism for
804 *Cryptococcus neoformans* Macrophage-to-Macrophage Transfer. *The Journal of Immunology*
805 ji1801118 (2019). [PMID:30877168]

806 **40**. Cherniak, R.; Valafar, H.; Morris, L. C.; Valafar, F. Cryptococcus neoformans chemotyping by
807 quantitative analysis of 1H NMR spectra of glucuronoxylomannans using a computer simulated
808 artificial neural network. *Clin. Diagn. Lab. Immunol* **5**, 146–159 (1998).

809 **41**. Westman, J.; Moran, G.; Mogavero, S.; Hube, B.; Grinstein, S. Candida albicans Hyphal Expansion
810 Causes Phagosomal Membrane Damage and Luminal Alkalinization. *MBio* **9**, (2018).
811 [PMID:30206168]

812 **42**. Weber, S. M.; Levitz, S. M. Chloroquine antagonizes the proinflammatory cytokine response to
813 opportunistic fungi by alkalizing the fungal phagolysosome. *J Infect Dis* **183**, 935–942 (2001).
814 [PMID:11237811]

815 **43**. Harrison, T. S.; Griffin, G. E.; Levitz, S. M. Conditional lethality of the diprotic weak bases
816 chloroquine and quinacrine against Cryptococcus neoformans. *J. Infect. Dis* **182**, 283–289 (2000).

817 **44**. Artavanis-Tsakonas, K.; Love, J. C.; Ploegh, H. L.; Vyas, J. M. Recruitment of CD63 to Cryptococcus
818 neoformans phagosomes requires acidification. *Proc. Natl. Acad. Sci. U. S. A* **103**, 15945–15950
819 (2006).

820 **45**. Mantegazza, A. R.; Savina, A.; Vermeulen, M.; Pérez, L.; Geffner, J.; Hermine, O.; Rosenzweig, S.
821 D.; Faure, F.; Amigorena, S. NADPH oxidase controls phagosomal pH and antigen cross-
822 presentation in human dendritic cells. *Blood* **112**, 4712–4722 (2008). [PMID:18682599]

823 **46**. Savina, A.; Jancic, C.; Hugues, S.; Guermonprez, P.; Vargas, P.; Moura, I. C.; Lennon-Duménil, A.-
824 M.; Seabra, M. C.; Raposo, G.; Amigorena, S. NOX2 Controls Phagosomal pH to Regulate Antigen
825 Processing during Crosspresentation by Dendritic Cells. *Cell* **126**, 205–218 (2006).

826 **47**. Yates, R. M.; Russell, D. G. Phagosome Maturation Proceeds Independently of Stimulation of Toll-
827 like Receptors 2 and 4. *Immunity* **23**, 409–417 (2005).

828 **48**. Rathman, M.; Sjaastad, M. D.; Falkow, S. Acidification of phagosomes containing Salmonella
829 typhimurium in murine macrophages. *Infect Immun* **64**, 2765–2773 (1996). [PMID:8698506]

830 **49**. Queval, C. J.; Brosch, R.; Simeone, R. The Macrophage: A Disputed Fortress in the Battle against
831 Mycobacterium tuberculosis. *Front Microbiol* **8**, 2284 (2017). [PMID:29218036]

832 **50**. Gillard, J. J.; Laws, T. R.; Lythe, G.; Molina-Paris, C. Modeling early events in Francisella tularensis
833 pathogenesis. *Front Cell Infect Microbiol* **4**, 169 (2014). [PMID:25566509]

834 **51**. Darwin, C. *The Foundation of the Origin of Species: Two Essays Written in 1842 and 1844.* ;
835 Cambridge University Press: Cambridge, UK, 1909

836 **52**. Slatkin, M. Cascading speciation. *Nature* **252**, 701–702 (1974). [PMID:4437620]

837 **53**. Philippi, T.; Seger, J. Hedging one's evolutionary bets, revisited. *Trends Ecol Evol* **4**, 41–44 (1989).
838 [PMID:21227310]

839 **54**. Bergman, A. . T. M. On the Natural Selection of Market Choice. *Autonomous Agents and Multi-*
840 *Agent Systems* **5**, 387–395 (2002).

841 **55**. Olofsson, H.; Ripa, J.; Jonzén, N. Bet-hedging as an evolutionary game: the trade-off between egg
842 size and number. *Proceedings. Biological sciences* **276**, 2963–2969 (2009). [PMID:19474039]

843 **56**. Heiple, J. M.; Taylor, D. L. pH changes in pinosomes and phagosomes in the ameba, Chaos
844 carolinensis. *The Journal of Cell Biology* **94**, 143–149 (1982). [PMID:7119011]

845 **57**. Watts, C.; Marsh, M.; Martin, J. B.; Satre, M.; Martin, J. B.; Satre, M. Endocytosis: what goes in
846 and how? *Journal of cell science* **103 (Pt 1)**, 1–8 (1992). [PMID:1429899]

847 **58**. Curran, R. E.; Claxton, C. R. J.; Hutchison, L.; Harradine, P. J.; Martin, I. J.; Littlewood, P. Control
848 and Measurement of Plasma pH in Equilibrium Dialysis: Influence on Drug Plasma Protein
849 Binding. *Drug Metabolism and Disposition* **39**, 551–557 (2011). [PMID:21098647]

850 **59**. Davis, M. J.; Tsang, T. M.; Qiu, Y.; Dayrit, J. K.; Freij, J. B.; Huffnagle, G. B.; Olszewski, M. A.
851 Macrophage M1/M2 polarization dynamically adapts to changes in cytokine microenvironments
852 in Cryptococcus neoformans infection. *mBio* **4**, e00264-00213 (2013). [PMID:23781069]

853 **60**. Leopold Wager, C. M.; Wormley, F. L. Classical versus alternative macrophage activation: the Ying
854 and the Yang in host defense against pulmonary fungal infections. *Mucosal Immunology* **7**, 1023–
855 1035 (2014). [PMID:25073676]

856 **61**. Leung, C.-Y.; Palmer, L. C.; Kewalramani, S.; Qiao, B.; Stupp, S. I.; Olvera de la Cruz, M.; Bedzyk, M.
857 J. Crystalline polymorphism induced by charge regulation in ionic membranes. *Proceedings of the*
858 *National Academy of Sciences of the United States of America* **110**, 16309–16314 (2013).
859 [PMID:24065818]

860 **62**. Jacobsohn, M. K.; Lehman, M. M.; Jacobsohn, G. M. Cell membranes and multilamellar vesicles:
861 Influence of pH on solvent induced damage. *Lipids* **27**, 694–700 (1992).

862 **63**. Weber, S. M.; Levitz, S. M.; Harrison, T. S. Chloroquine and the fungal phagosome. *Current*
863 *Opinion in Microbiology* **3**, 349–353 (2000).

864 **64**. Casadevall, A.; Pirofski, L. A. What Is a Host? Attributes of Individual Susceptibility. *Infect Immun*
865 **86**, (2018). [PMID:29084893]

866 **65**. Kulp, C. W.; Zunino, L. Discriminating chaotic and stochastic dynamics through the permutation
867 spectrum test. *Chaos* **24**, 33116 (2014). [PMID:25273196]

868

869

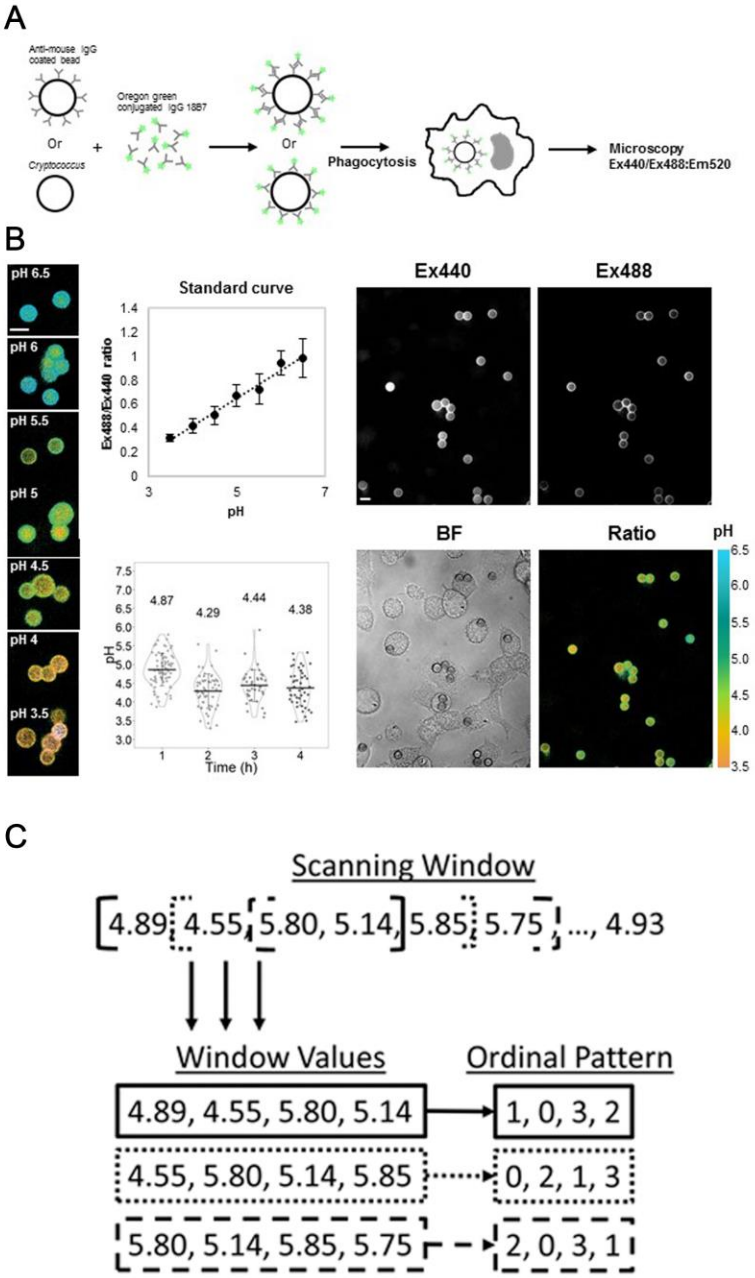

Figure 1. Experimental designs for described methods. **A.** Experimental design for phagolysosomal pH measurement. Particles are opsonized with mAb 18B7 conjugated to fluorophore OregonGreen. **B.** Measurement of phagolysosomal pH. Measurements are based on ratiometric measuring of Ex440/Em520 and Ex488/Em520. **C.** Experimental design for the detection of Chaos within a system. A scanning window generates sets of windows values. Ordinal patterns are then generated by ordering the terms in each scanning window from least to greatest.

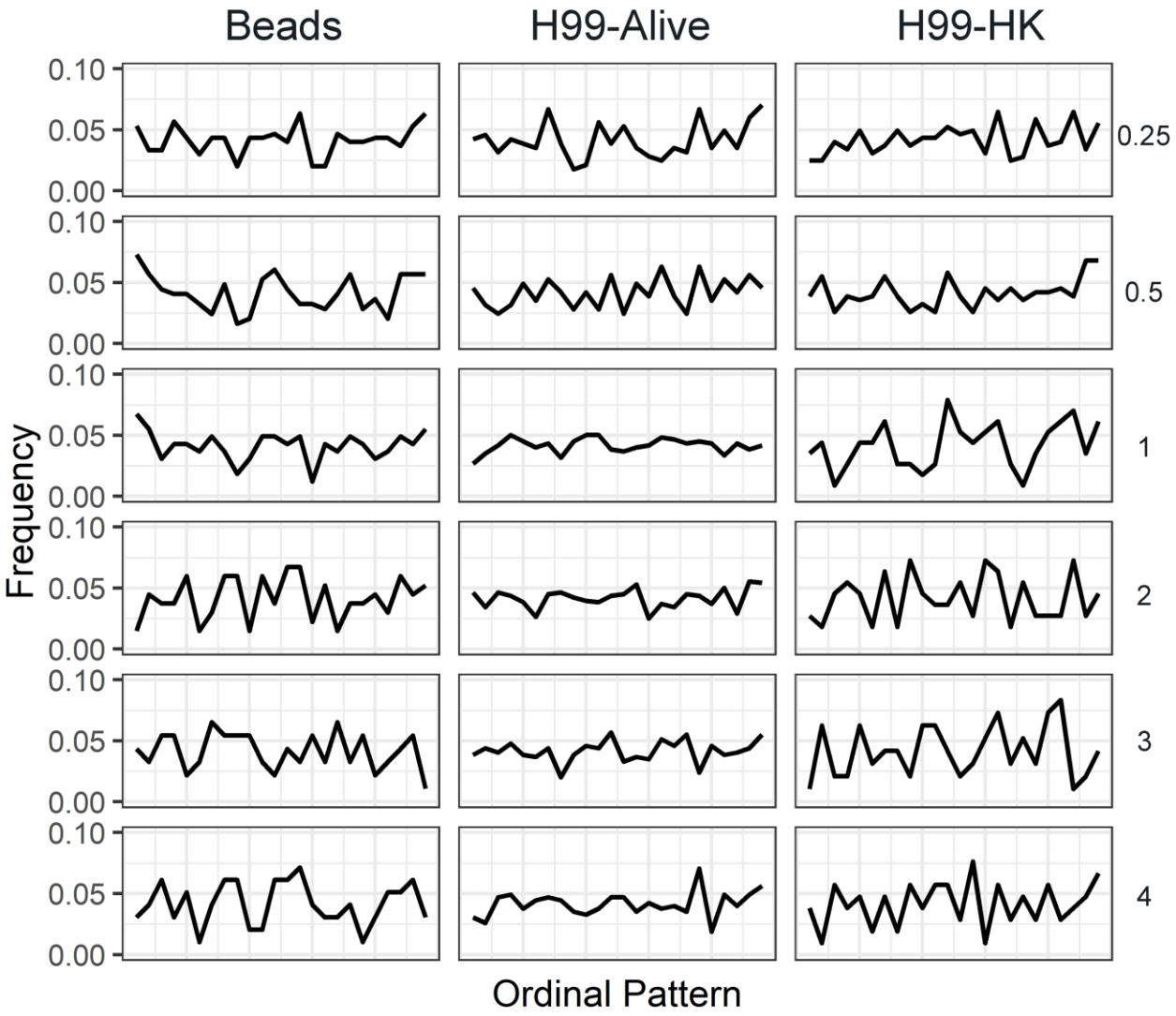

Figure 2. Murine macrophage phagolysosomes acidify stochastically. The frequency of each 4-unit ordinal pattern for each ingested particle: beads, live *C. neoformans*, and dead *C. neoformans* at various HPI. Note that all ordinal patterns have a non-zero frequency.

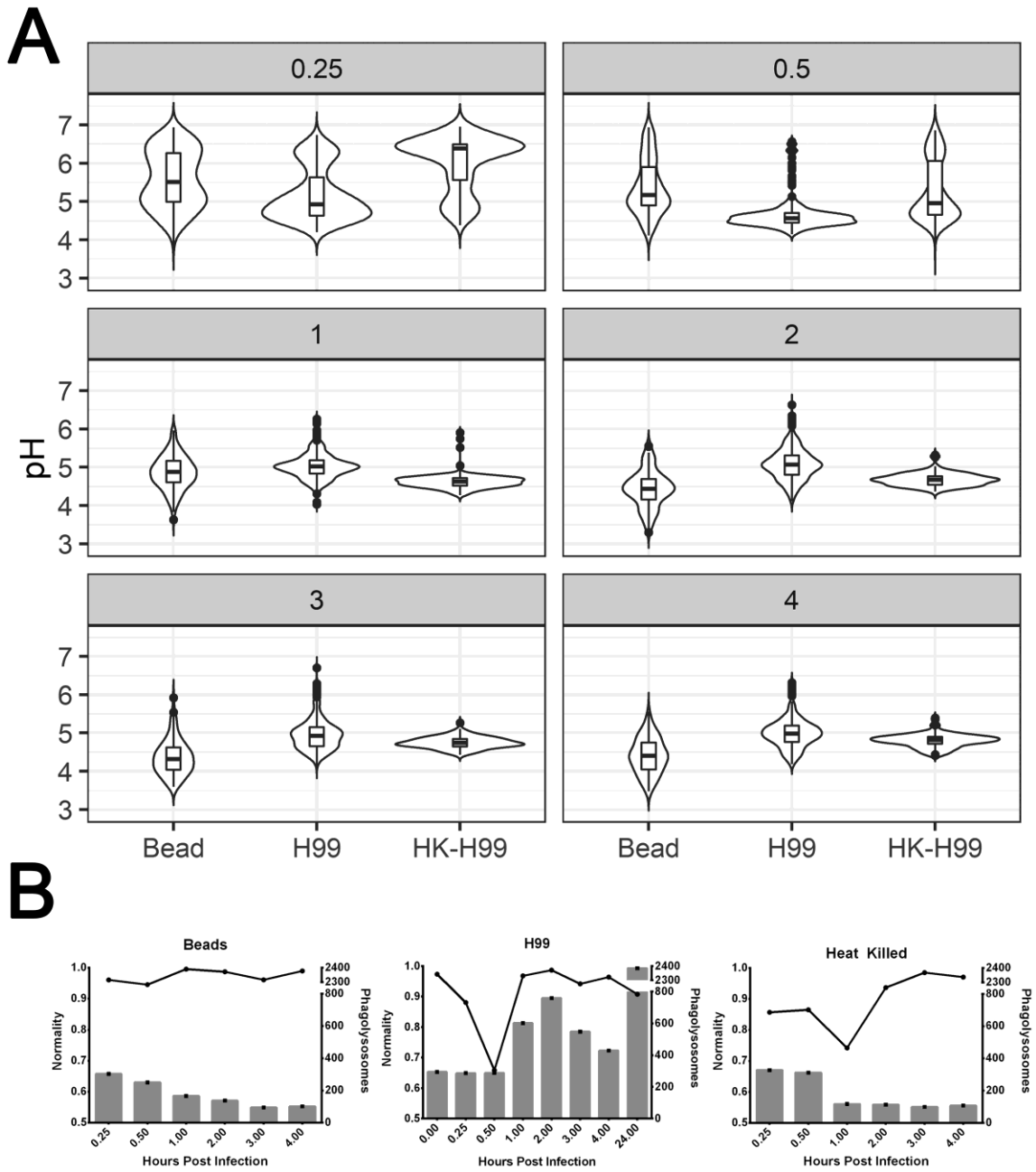

Figure 3. Bead ingested murine macrophage phagolysosomes stabilize to a normally distributed pH. **A.** Distributions of measured phagolysosomal pH after ingestion of various particles by BMDMs at various hours post infection (gray box value) for bead, live *C. neoformans* (H99), and dead *C. neoformans* (HK-H99). **B.** Visualization of estimated normality via Shapiro-Wilk (line) and total phagolysosome count (bar) for each sample.

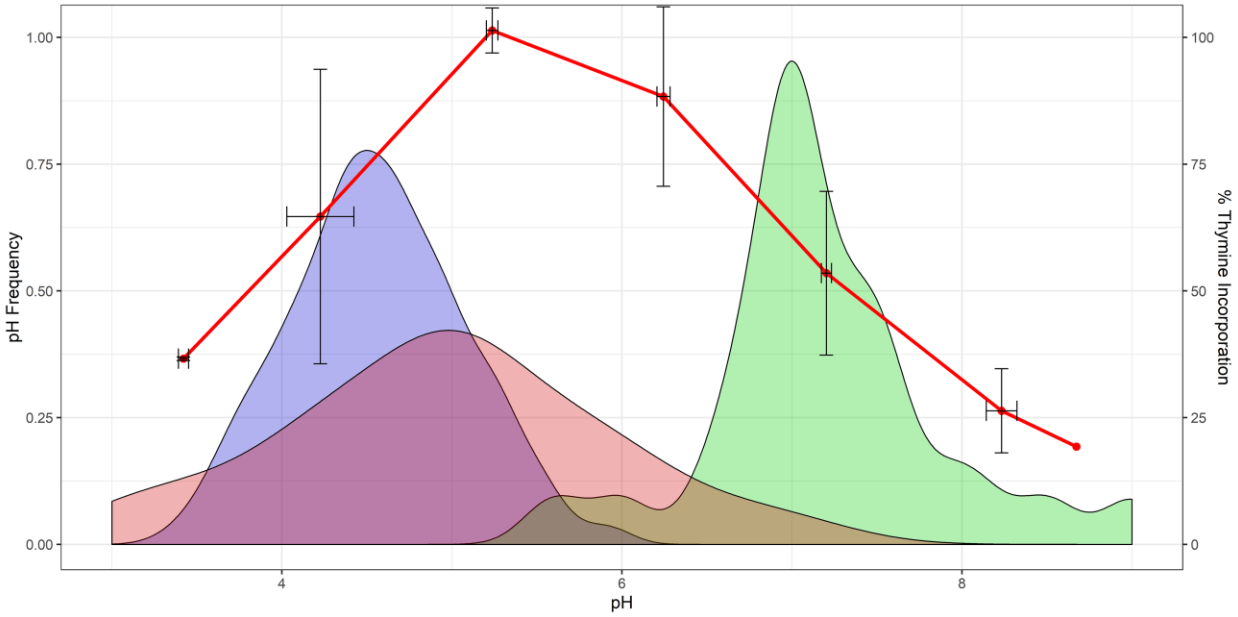

Figure 4. BMDM phagolysosomes acidify to a default pH range suboptimal for soil microbe and pathogen growth. Growth rates of soil bacteria[27,28] as percent thymine incorporation (red line) and distribution of minimal culturable pH for 27 human pathogens (red fill) compared to the distribution of observed phagolysosomal pH after bead ingestion and phagolysosome maturation, 1-4 HPI (blue fill). The bead pH distribution overlaps unfavorably with minimal growth conditions of microbes, and only minimally overlaps with the optimal growth pH range of the same 27 pathogens (green fill).

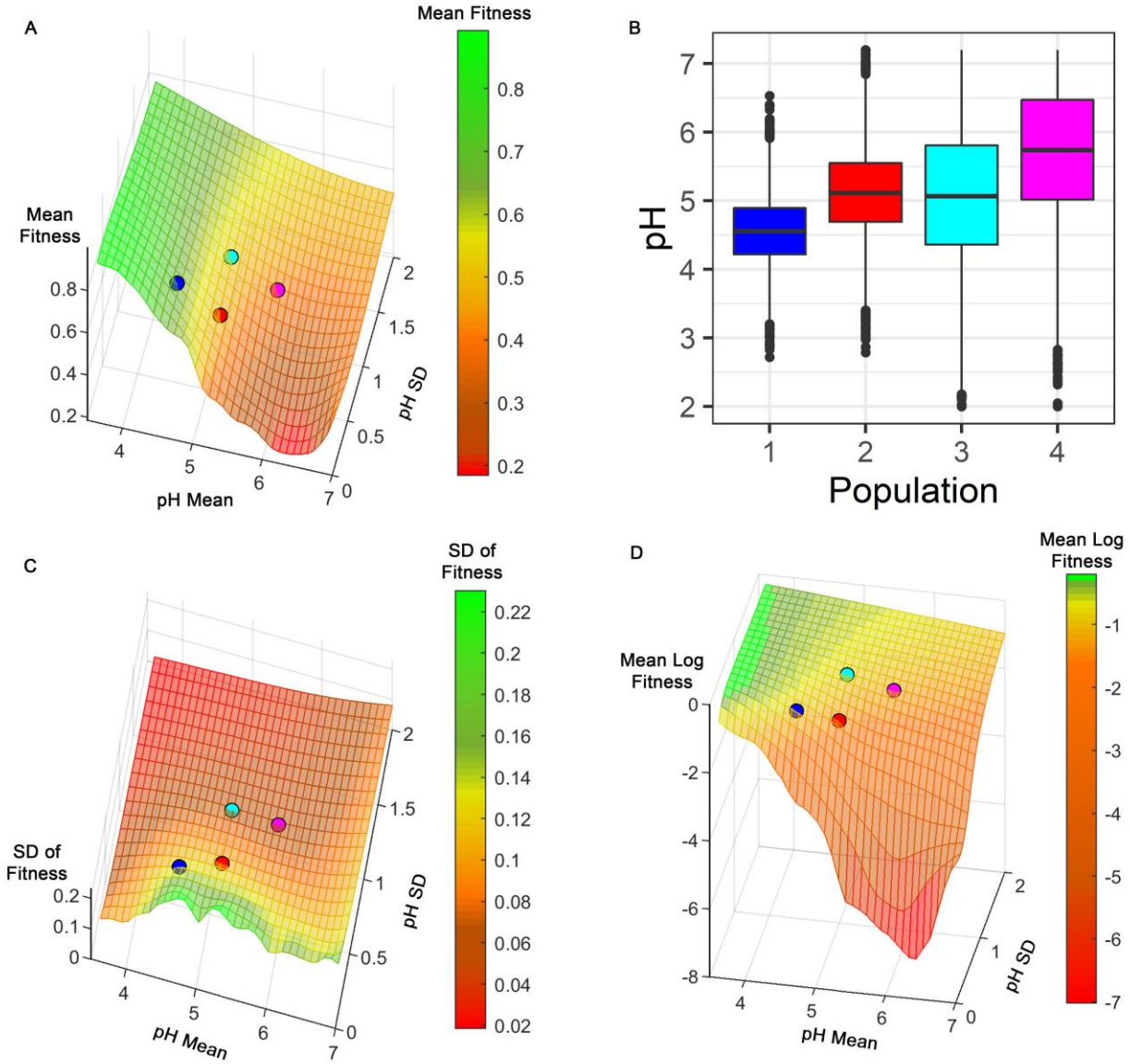

Figure 5. Simulated macrophage populations show stochastic pH as bet-hedging strategy. Success of host-microbe interactions are visualized as macrophage populations faced with randomly selected pathogens and acidified to random pHs from normal distributions of mean μ and standard deviation σ. Meshes represent host macrophage fitness, deviation in fitness, and log mean fitness. Plotted points represent measured data of H99 containing murine (red) and human (magenta) or bead containing murine (blue) and human (cyan) phagolysosomes. **A.** Mean macrophage survival (Z axis, colorbar) increases significantly as pH lowers, and mostly unchanged with standard deviation. **B.** Examples of simulated populations based on colored points in panel A. Each combination of mean and SD from the axes of panel A represent a unique population of macrophages with a fitness represented by the Z axis and colored mesh. **C.** Deviation in host fitness (Z axis, colorbar) dramatically decreases by increasing standard deviation of pH, and mostly unaffected by shifts in mean pH. **D.** Logarithmic measurement of host fitness (Z axis, colorbar) to observe long term trends applicable to a bet-hedging strategy.

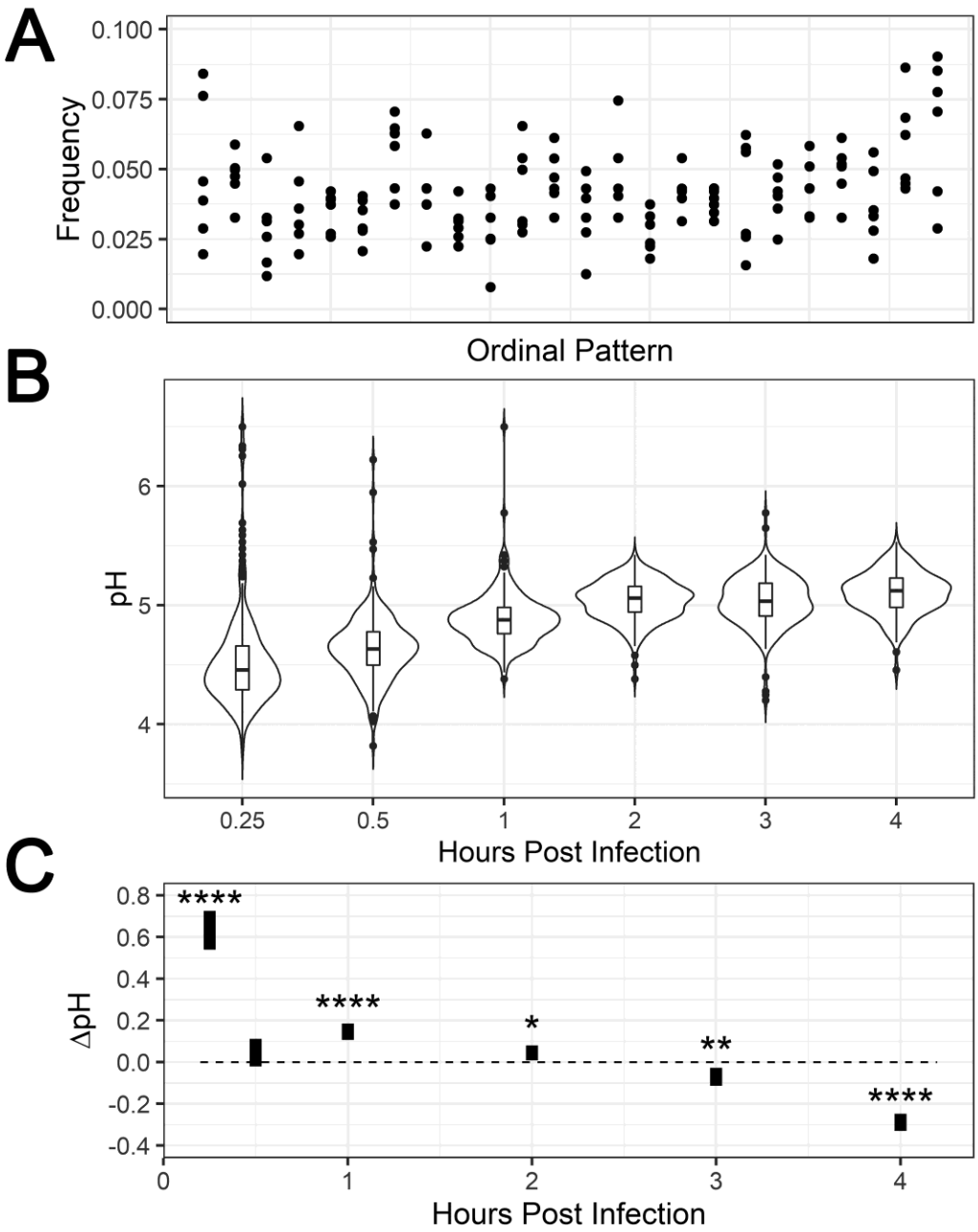

907

908 **Figure 6.** Trained murine macrophages have inverse acidification dynamics. **A.** Ordinal pattern analysis of
909 phagolysosome pH in trained BMDMs. All ordinal patterns appear at a non-zero frequency. **B.** pH
910 distributions of phagolysosomes at various HPI. **C.** Difference (95% CI) after subtracting mean trained
911 phagolysosome pH from mean untrained phagolysosome pH at each timepoint. *, **, **** denote $P <$
912 0.05, 0.01, and 0.0001 respectively via two tailed t-test.

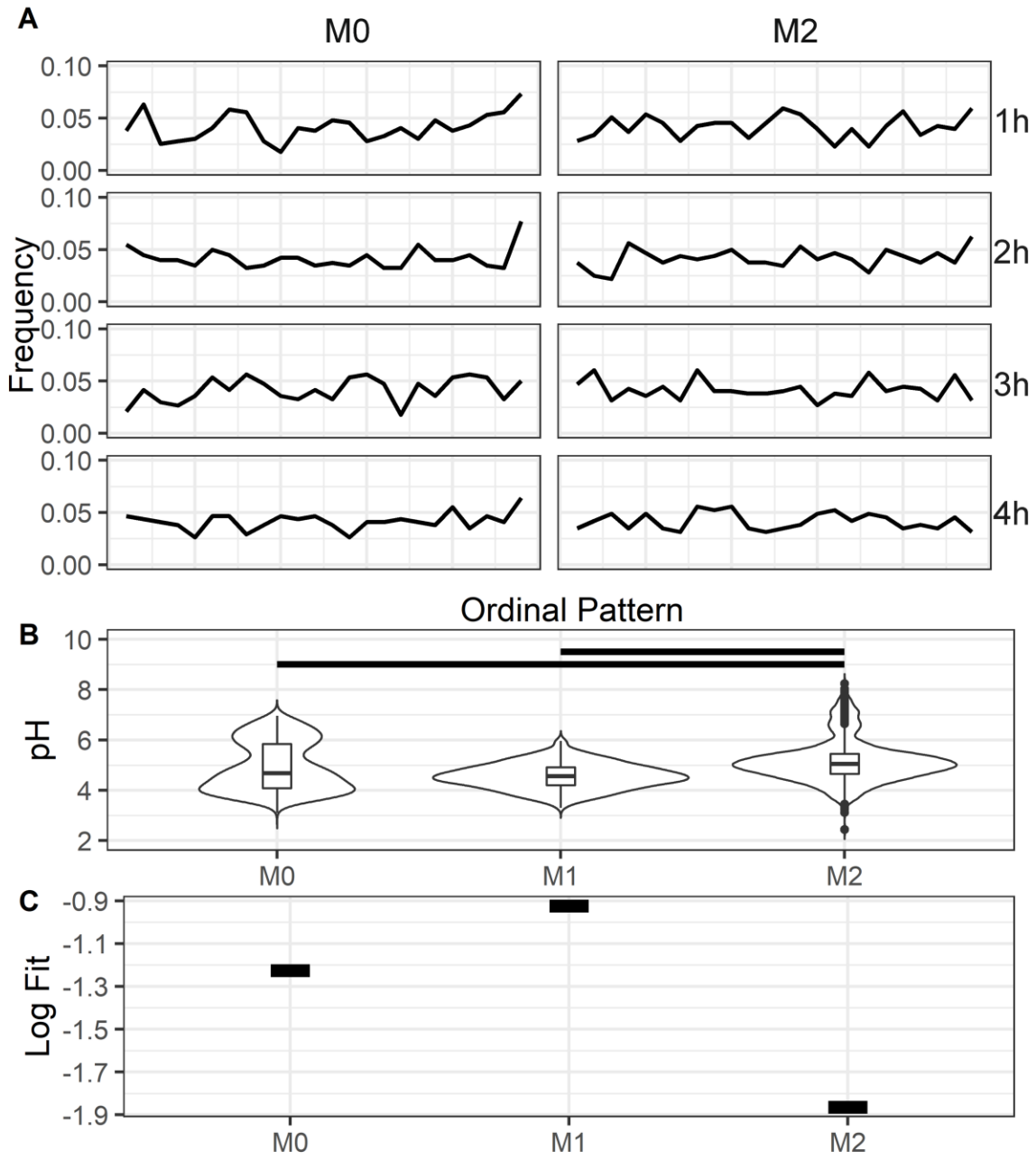

Figure 7. Phagolysosome dynamics of macrophages skewed toward different polarization states. **A.** Ordinal patterns of bead containing phagolysosomes at various HPI. **B.** Bead containing phagolysosome pH distributions of differently polarized macrophages. Black bars represent $P < 0.0001$ via Kruskal-Wallis test with Wilcox rank pairing test. **C.** Mean log fitness of bead containing phagolysosomes according to our bet hedging model.

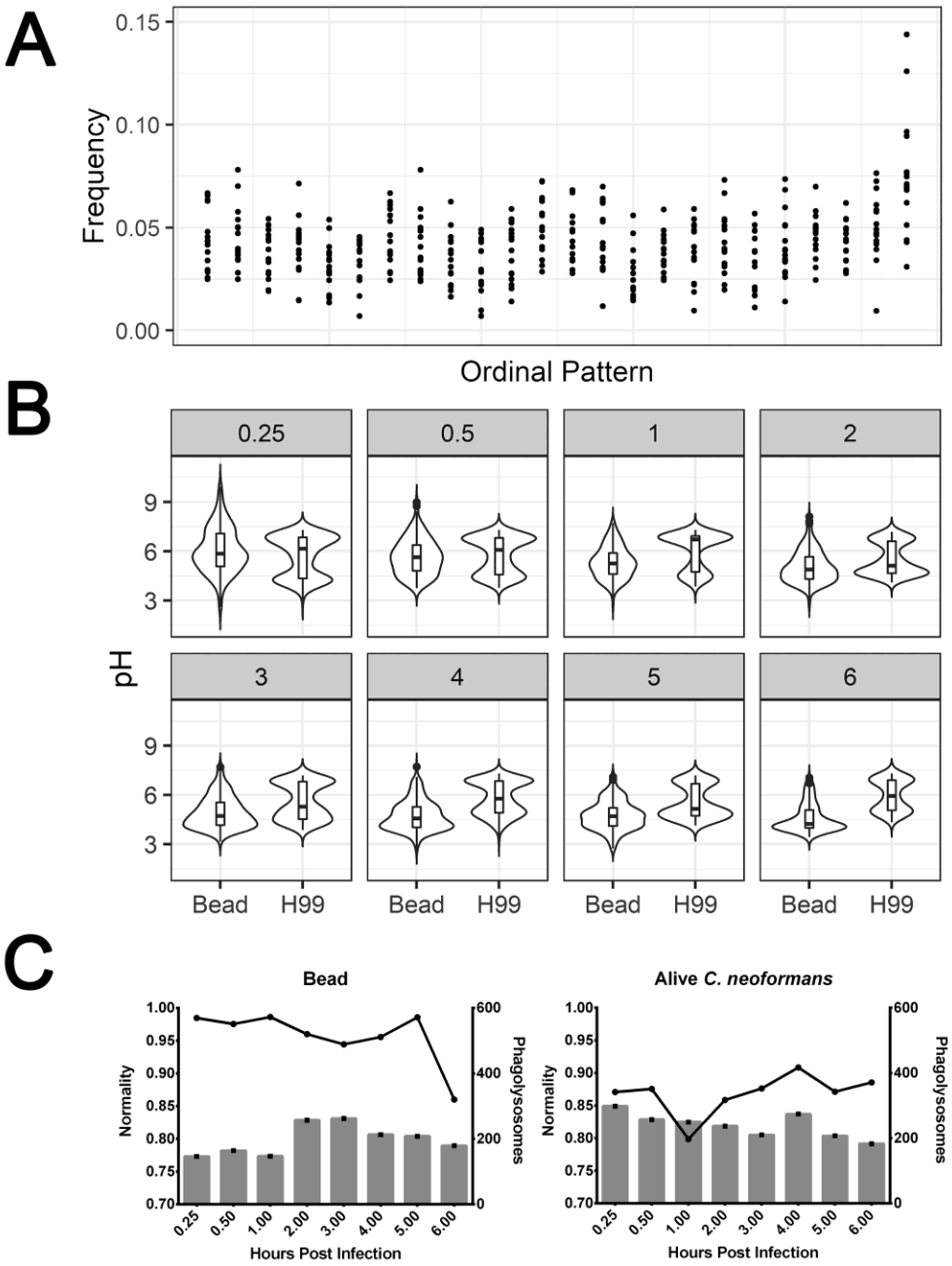

Figure 8. Isolated human monocytes acidify stochastically and approximate normality. Human macrophages were infected with inert beads or live *C. neoformans*, and their pH analyzed at various timepoints. **A.** Ordinal Pattern analysis for all conditions. All patterns exist at non-zero frequencies for all timepoints. **B.** Distributions of phagolysosome pH at different timepoints. **C.** Shapiro-Wilk normality and total sample count for each condition.

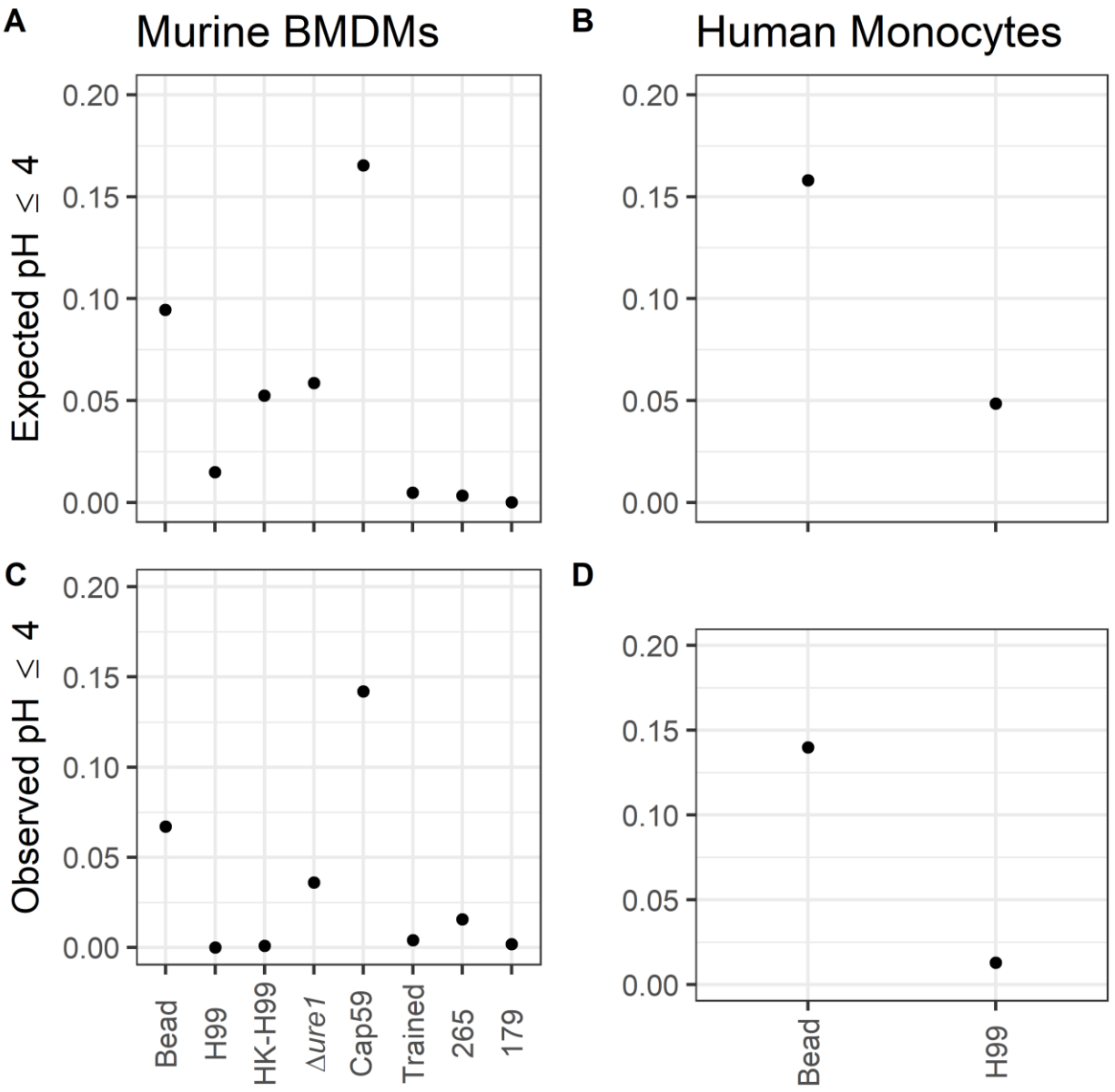

Figure 9. Expected and observed likelihood of phagolysosomes to achieve pH ≤ 4. **A.** The expected proportions of murine BMDM phagolysosomes to achieve pH ≤ 4 assuming a normal distribution based on all observed data. **B.** The expected proportions of human macrophage phagolysosomes to achieve pH ≤ 4 assuming a normal distribution based on the observed data. Expected proportions of macrophages to achieve pH ≤ 4 were calculated by assuming a normal distribution centered around a mean and standard deviation calculated from the observed data. **C.** The observed proportions of murine BMDM phagolysosomes to achieve pH ≤ 4. **D.** The observed proportions of human macrophage phagolysosomes to achieve pH ≤ 4.

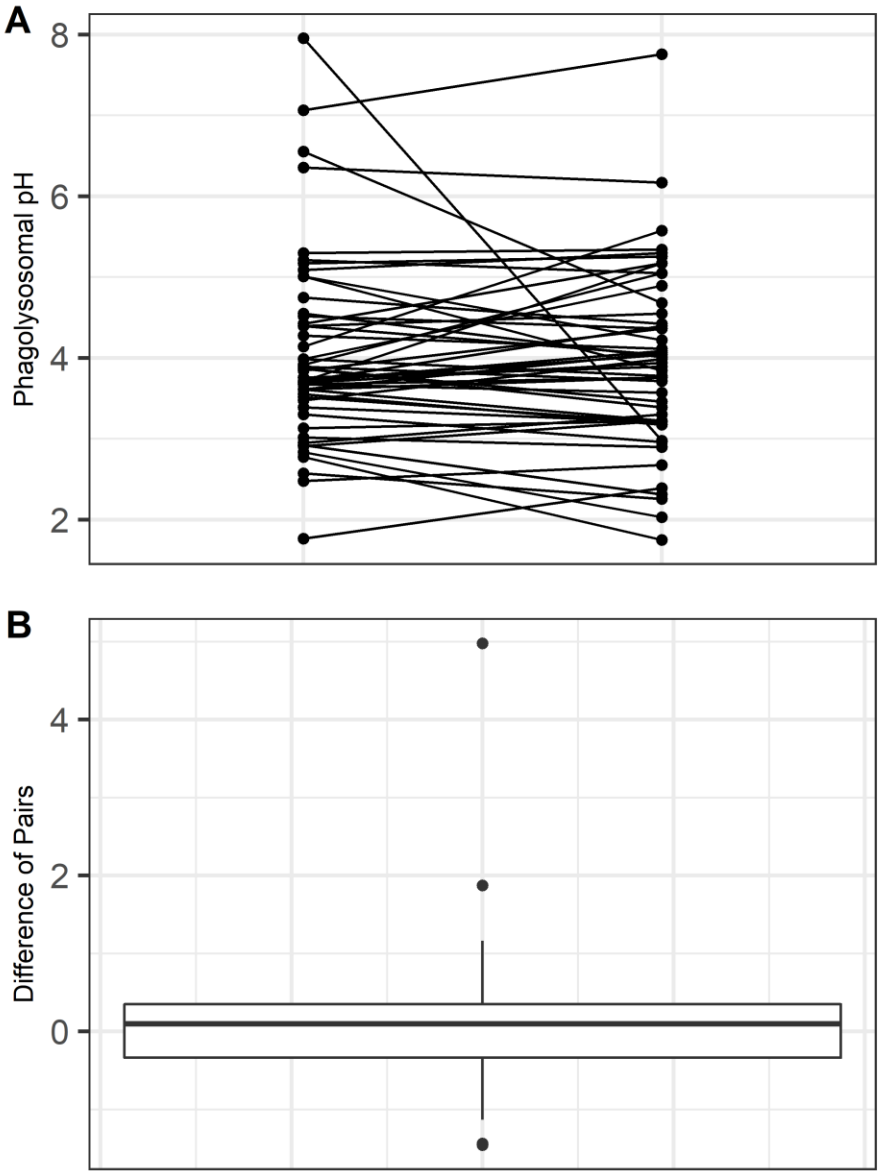

935

936 **Supplemental Figure 1.** Analysis of 80 pairs of phagolysosomes within single cells. **A.** Measured
937 phagolysosomal pH of multiple beads located in the same macrophage but non-proximal
938 phagolysosomes. Lines indicate particles within the same macrophage. Phagolysosomes were measured
939 in no particular order. **B.** Differences of each phagolysosomal pH pair approximate a normal distribution
940 centered around 0 with non-zero values despite being generated within the same macrophage at a
941 synchronized starting time.

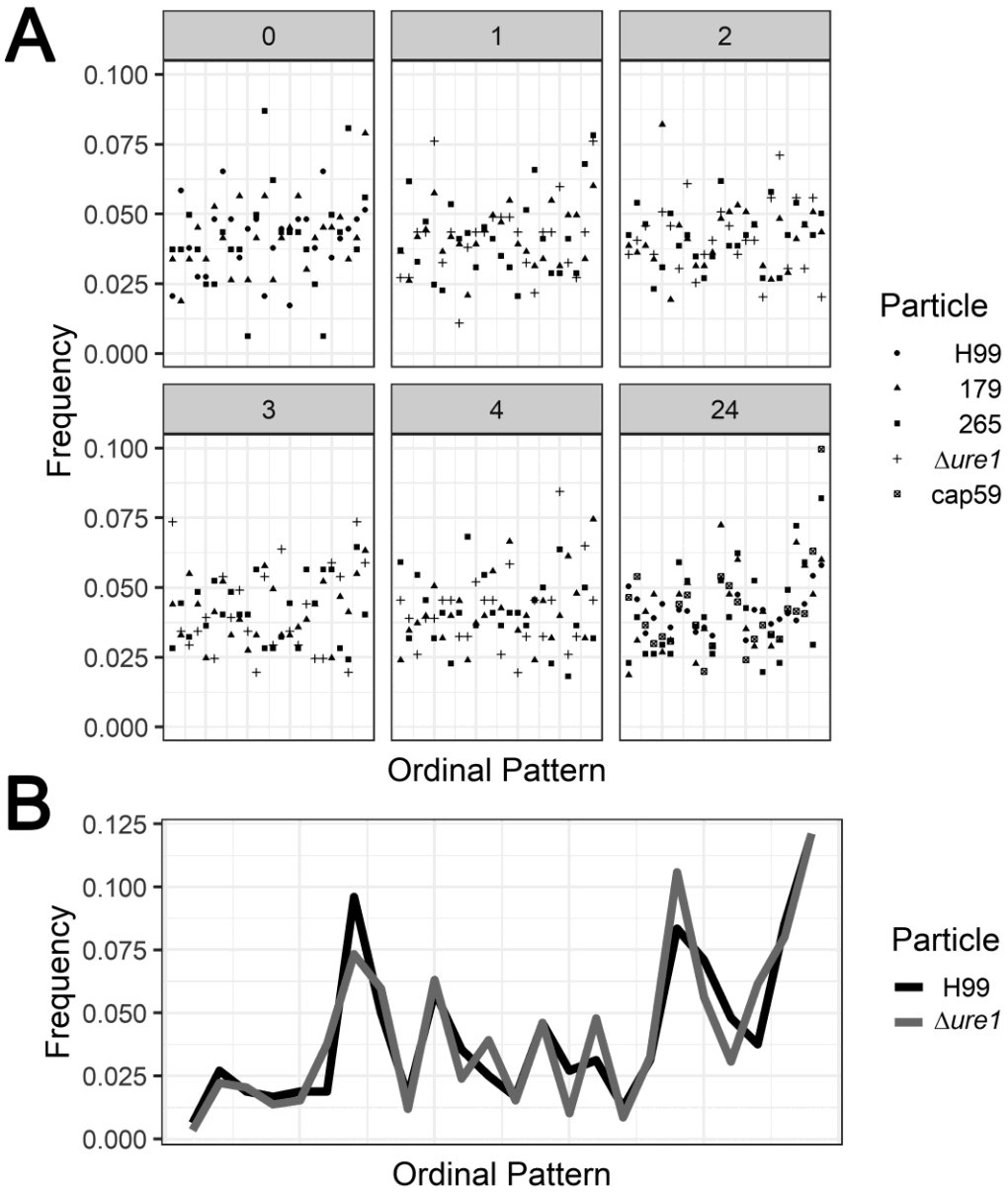

942

943 **Supplemental Figure 2.** Ordinal pattern analysis for expanded samples. **A.** Ordinal pattern frequencies for
944 phagolysosomal acidification intervals in BMDMs infected with various particles at various hours post
945 infection (gray box values). **B.** Ordinal pattern frequencies for time elapsed before initiation of budding
946 for yeast strains ingested by BMDMs.

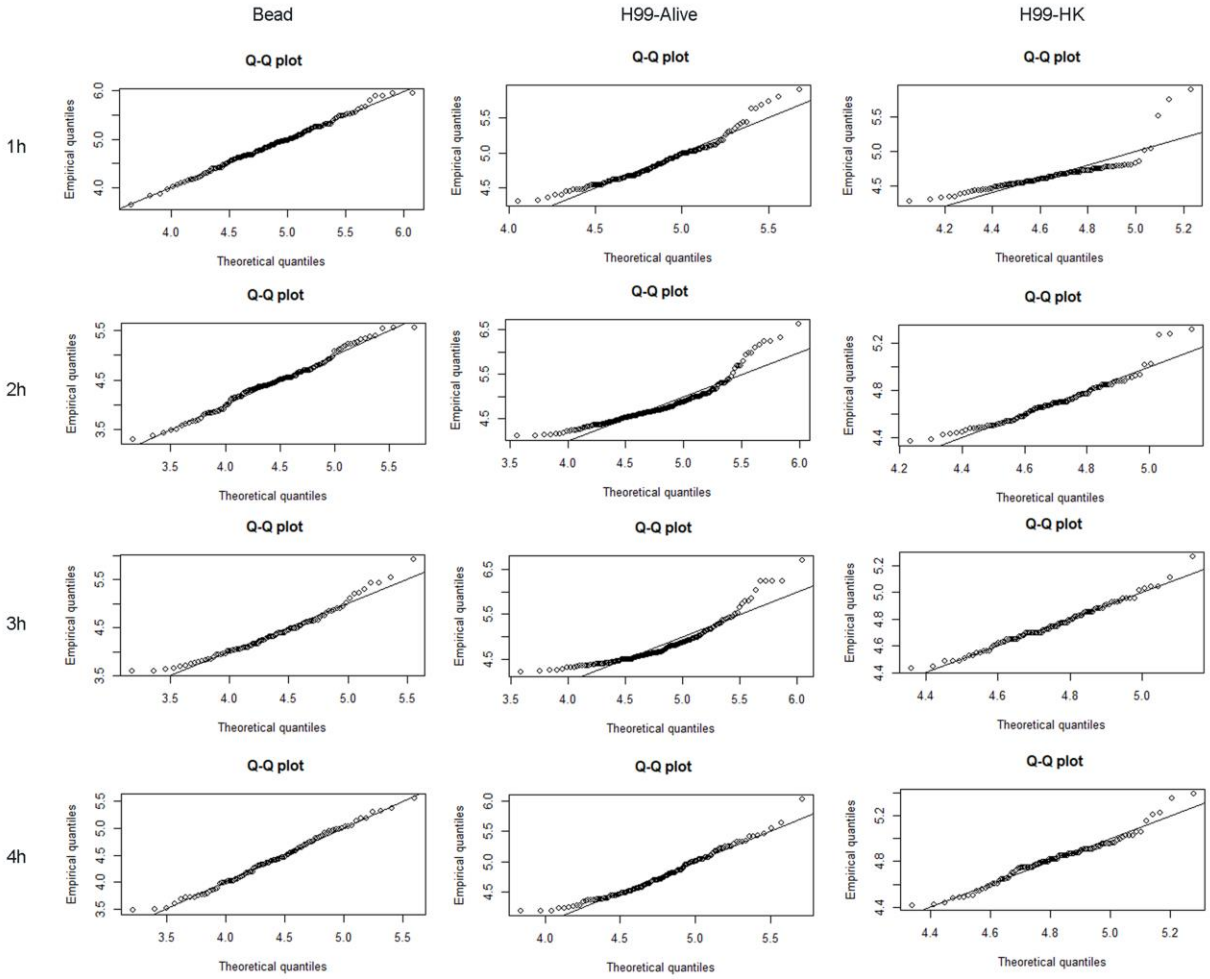

947

948 **Supplemental Figure 3.** Q-Q plots of macrophages 1-4 HPI after ingesting various particles. Note that bead
949 containing phagolysosomes closely approximate a normal distribution, while *C. neoformans* containing
950 phagolysosomes have heavy tails, regardless if the particle is live or dead.

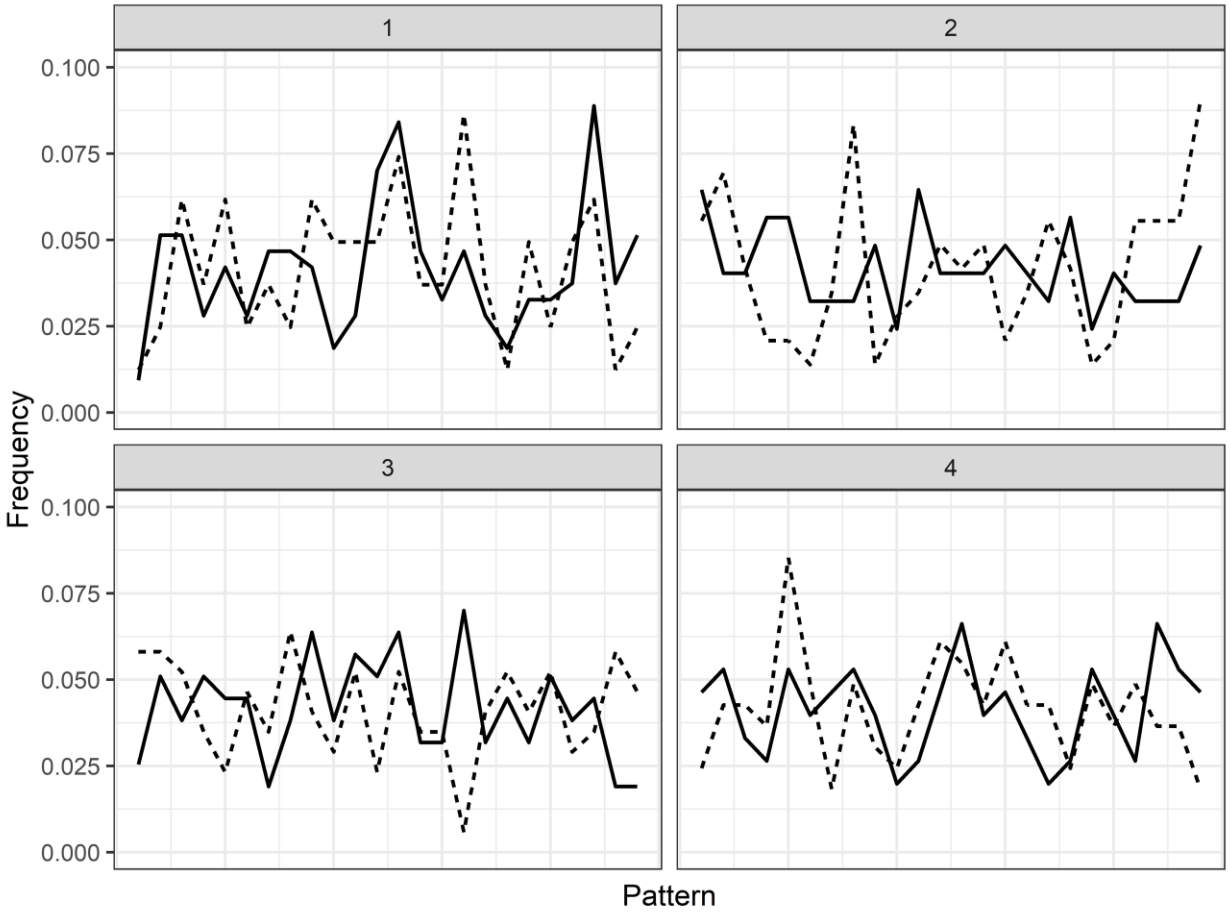

Supplemental Figure 4. Ordinal pattern analysis for EEA1 (solid) and VATPase (dashed) immunofluorescent staining for bead containing macrophage phagolysosomes at various hours post ingestion (gray box values). No forbidden ordinal patterns were detected for any samples, suggesting phagolysosomal maturation marker acquisition is a stochastic process.

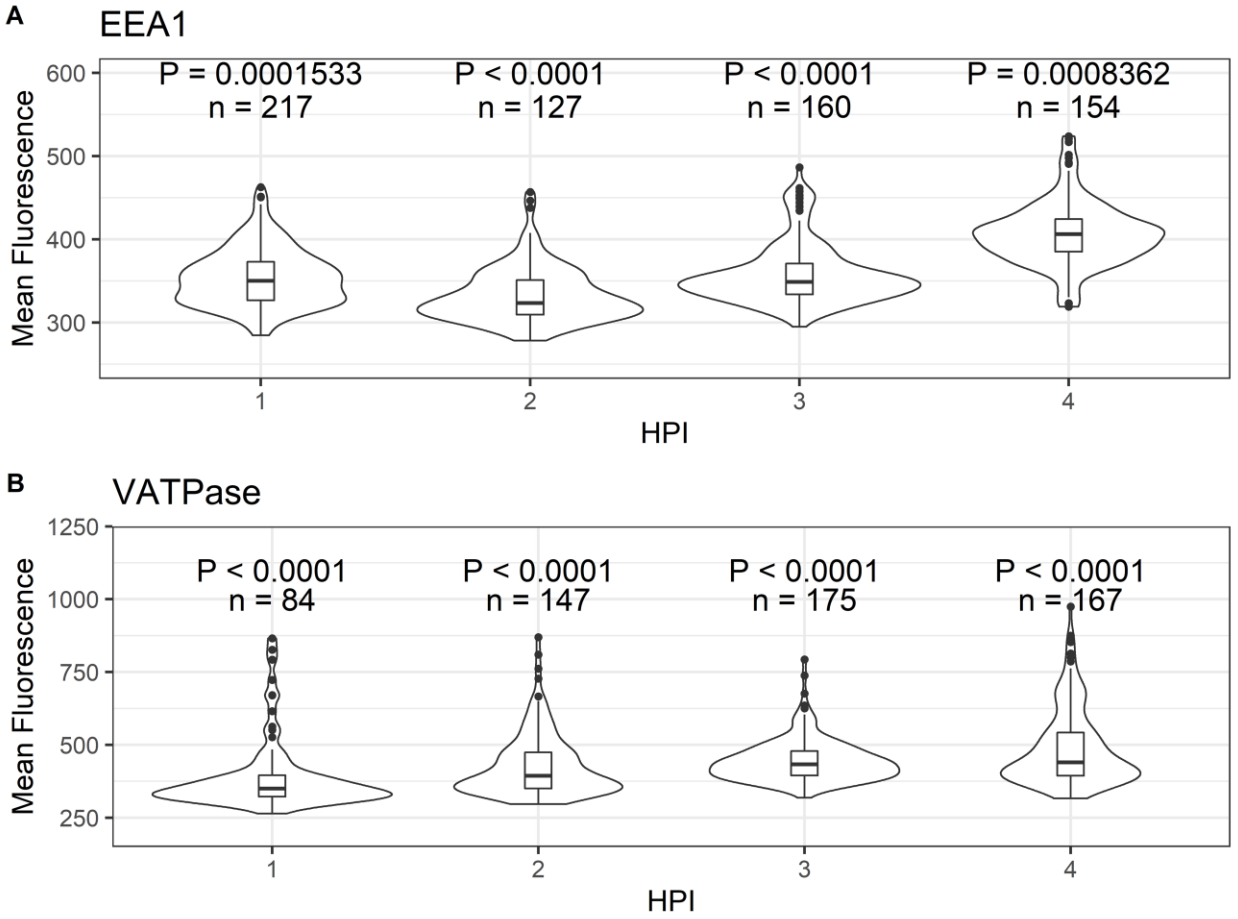

Supplemental Figure 5. Mean fluorescence intensity values for EEA1 and VATPase immunofluorescent staining. The acquisition of these phagolysosomal maturation markers does not resemble that of bead containing phagolysosomal pH, as no samples here are normally distributed. P values were determined via Shapiro-Wilk normality test.

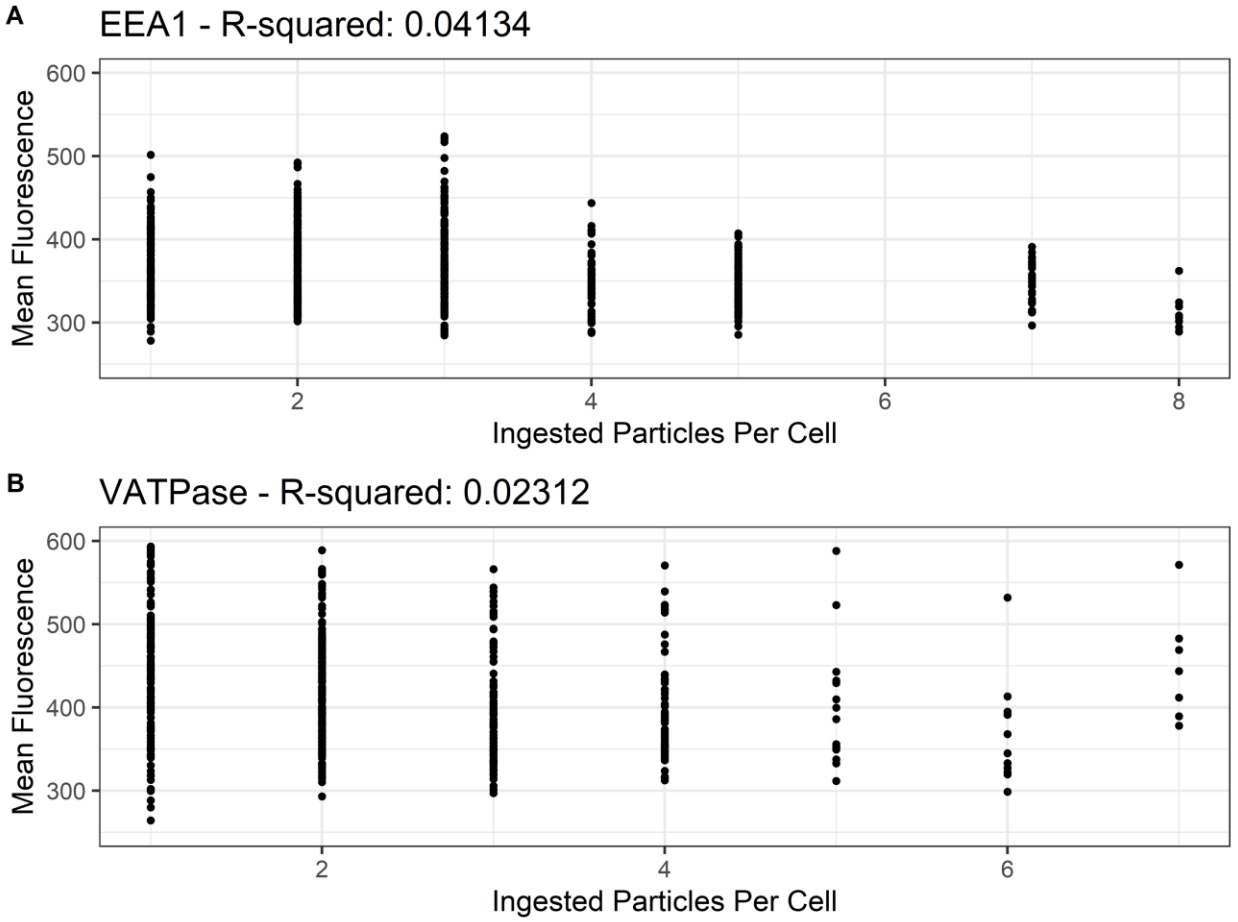

Supplemental Figure 6. Mean fluorescent intensity of macrophage ingested beads stained for EEA1 and VATPase, sorted according to total ingested particles per cell. Linear regressions were calculated for each sample set but clearly there is no significant correlation between total ingested particles and number of EEA1 or VATPase molecules as measured by fluorescent intensity.

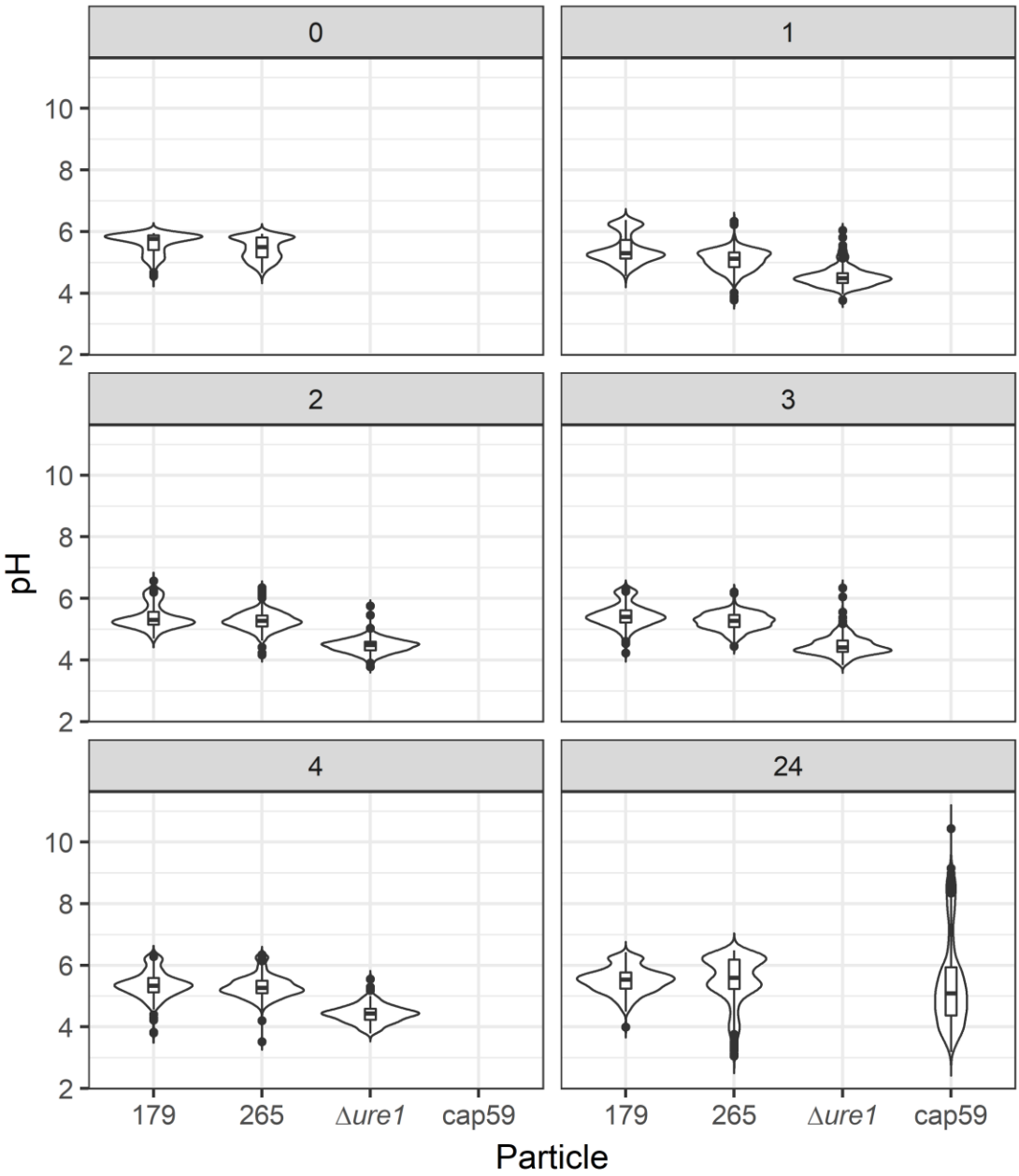

Supplemental Figure 7. Phagolysosomal pH distributions for expanded samples. Two strains of *C. gattii* (179 and 265), a urease deficient H99 mutant (*Δure1),* and a capsule deficient H99 mutant (cap59) were analyzed at various hours post infection (gray box value).

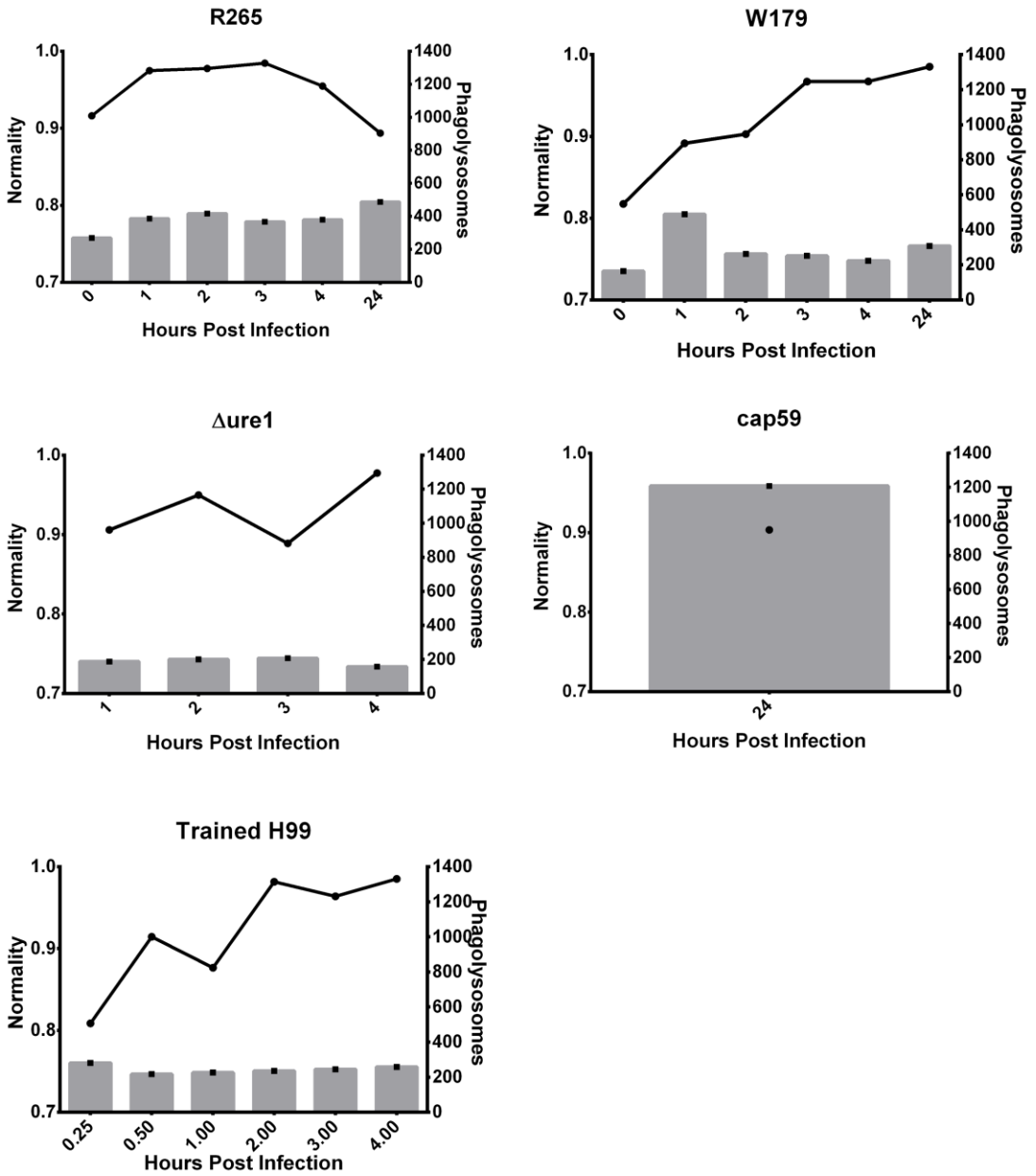

970

971 **Supplemental Figure 8.** Normality analysis for expanded samples. Shapiro-Wilk normality values (lines)
972 alongside total phagolysosome sample sizes (bars) for two strains of *C. gattii* (179 and 265), a urease
973 deficient H99 mutant (*Δure1),* a capsule deficient H99 mutant (cap59), and trained BMDMs on reinfection.

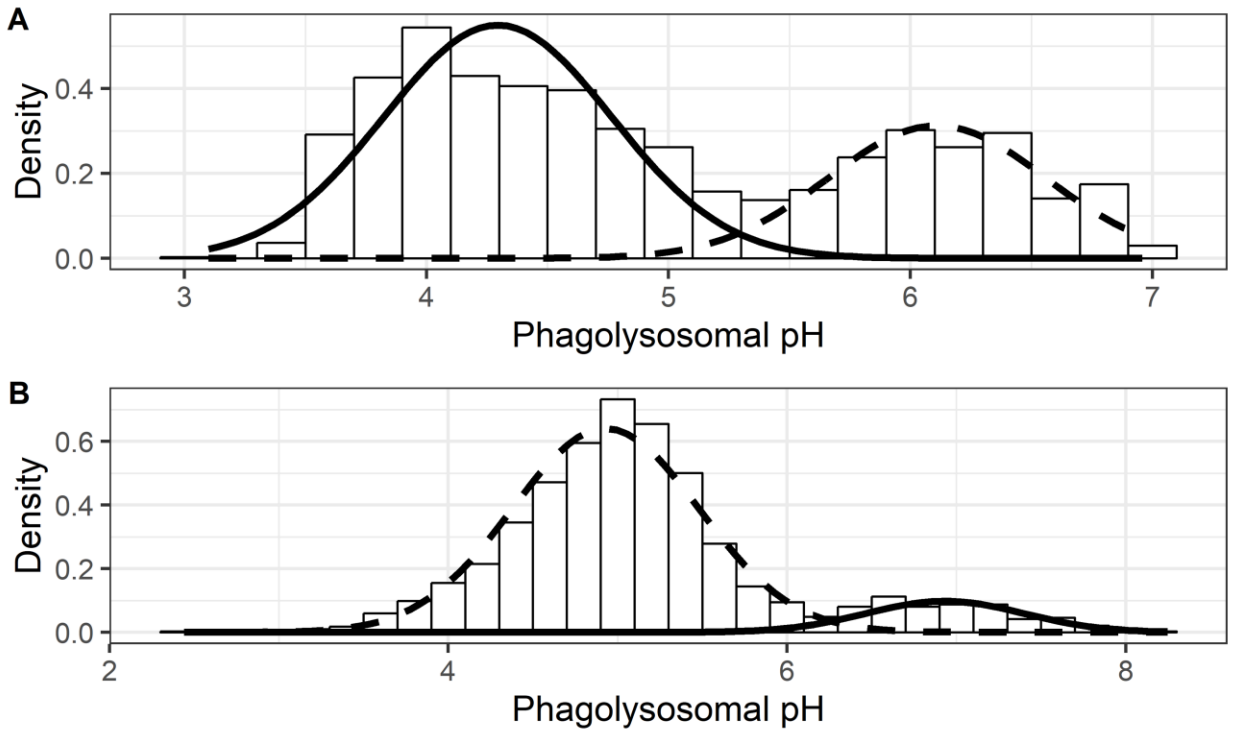

Supplemental Figure 9. Bimodal models fitted to the observed data for **A.** M0 and **B.** M2 skewed macrophages. Models are attempted fits of two mixed Gaussian distributions. Histogram bars visualize the observed data while solid and dashed lines depict the relative contributions of the two hypothetical Gaussian distributions.

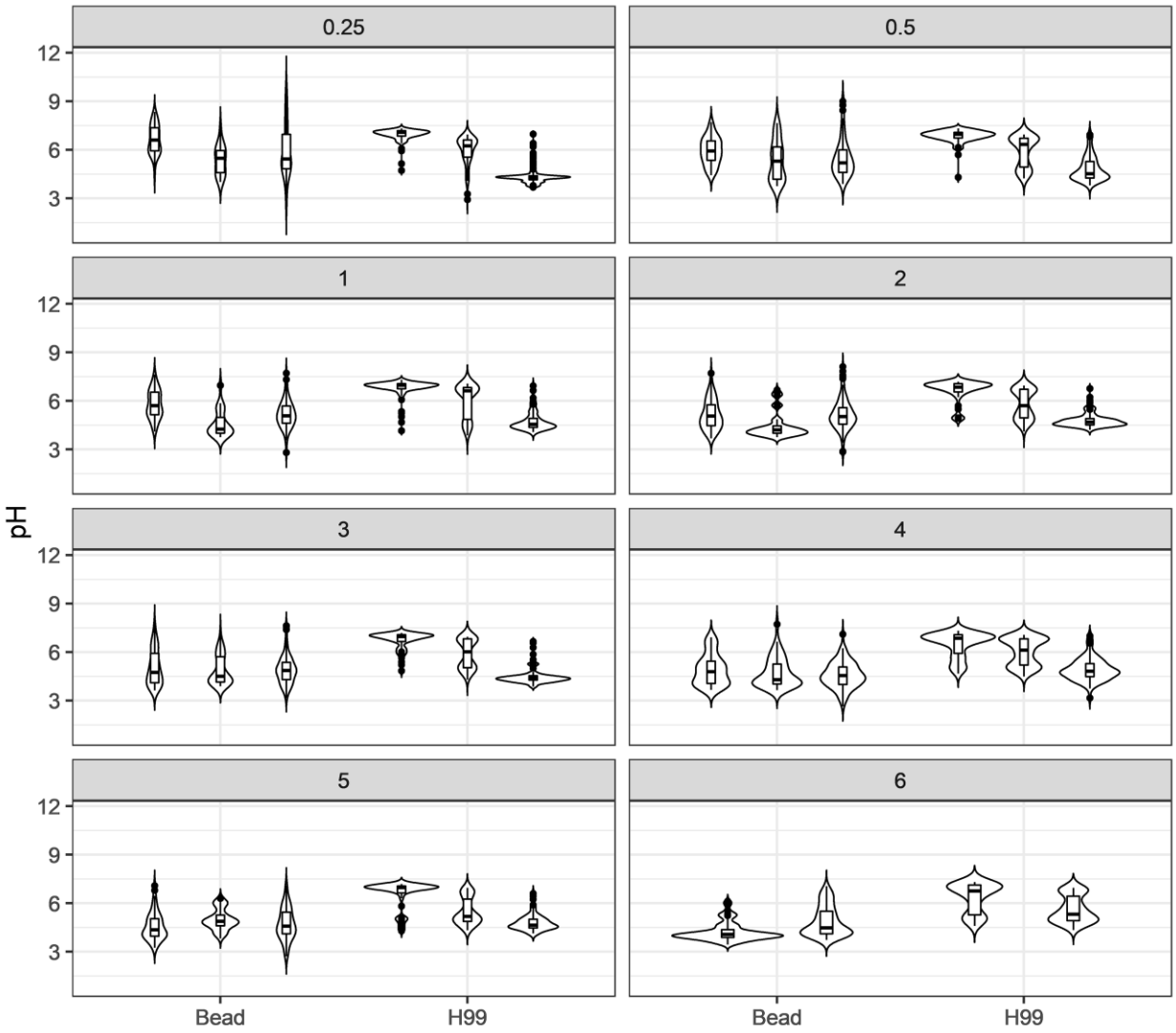

979

980 **Supplemental Figure 10.** Phagolysosomal pH distributions for human macrophages infected with H99
981 separated by individual donor. Human macrophages were analyzed after ingesting either H99 or inert
982 beads at various hours post infection (gray box value).

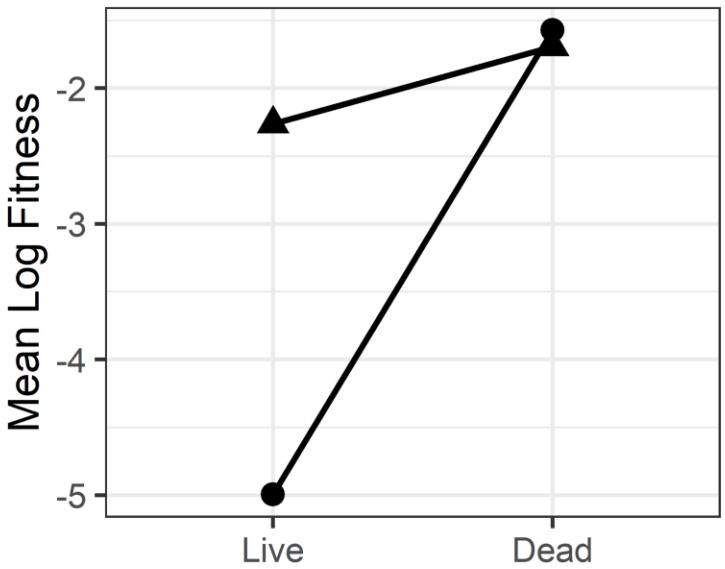

983

984 **Supplemental Figure 11.** Estimated mean log fitness of macrophages containing live or killed *M. avium*.
985 Phagolysosomal pH data was gathered from literature using either video microscopy (triangles) or
986 confocal microscopy (circles).